ESTEC/Contract No. 16361/02/NL/LvH
ESA Study on Magnetospheric Propulsion for Scientific Exploration (eMPii)

Magnetospheric Propulsion (eMPii)

Final report
Issue 1.3 April 5, 2004

Authors:
P. K. Toivanen, P. Janhunen, H. E. J. Koskinen*

Finnish Meteorological Institute, Space Research Unit, Helsinki
*also at: University of Helsinki, Department of Physical Sciences

ESA Technical Officer:
A. Hilgers
D/TOS Space Environments and Effects Analysis Section (TOS-EES)

Document status

1. Document Title: Magnetospheric Propulsion (eMPii)
2. Issue: 1
3. Revision: 3
4. Date: 05.04.04

Document change record

Issue:	Date:	Comments:
0.0	19.11.03	First draft for internal discussion
0.1	25.11.03	Revision of issue 0.0
0.2	26.11.03	Revision of issue 0.1, conclusions added
1.0	28.11.03	Draft report, submitted for approval
1.1	30.01.04	Revision of issue 1.0 reflecting requested revisions of WP300 and WP400 Technical Notes
1.2	15.03.04	Revision of issue 1.1 after ESTEC comments and detailed telephone discussion with A. Hilgers
1.3	05.04.04	Final, Accepted on 19.03.04 by A. Hilgers

Preface

This document is the final report of the ESTEC Contract No. 16361/02/NL/LvH – Magnetospheric Propulsion for Scientific Exploration. The document summarises the results of the project in a self-contained manner. In addition to this document the different technical work packages produced Technical Notes listed below. Furthermore an article on magnetospheric propulsion is to appear in the ESA journal "Preparing for the Future".

The study was conducted by a team at the Geophysical Research Division of the Finnish Meteorological Institute (FMI/GEO). The project manager was prof. Hannu Koskinen (also at the University of Helsinki, Deparment of Physical Sciences). Other members of the team were Dr. Pekka Janhunen and Dr. Petri Toivanen. The contract officer at FMI was Ms. Hanna Lappalainen.

According to the Statement of Work AO/1-4085/02/NL/LvH the main objective of the project was to investigate the theoretical issues related to the electrodynamic behaviour and their implications for the possible applications of the magnetospheric propulsion system and their technology requirements. The technical work to achieve this goal was divided in three work packages (WP200, WP300, WP400). The documents summarising the individual work packages are:

eMPii-FMI-TN-1: WP 200 Technical Note
Assessment of magnetospheric propulsion concept

eMPii-FMI-TN-2: WP 300 Technical Note
Parameter ranges and computer simulations for magnetic propulsion.

eMPii-FMI-TN-3: WP 400 Technical Note
Technology requirements for magnetospheric propulsion.

The Technical Notes are available upon request from ESTEC and the Contractor.

Acknowledgements

We wish to express our gratitude to the ESA Technical Officer of this project A. Hilgers for several intense discussions and patience with our study. We also thank Bengt Johlander for the information on semitransparent materials and temperatures feasible for the passive cooling of the superconductors in space. P. J. acknowledges his discussions with R. M. Winglee on the problems with M2P2. At the end this project turned out to be much more time consuming than anticipated in the project proposal. We are grateful to the Geophysical Research Division of the Finnish Meteorological Institute for the working environment where this was acceptable.

Abstract

Magnetospheric propulsion has been proposed as a revolutionary propulsion concept that could provide spacecraft with unprecedented speeds of 50 to 80 km s^{-1} or 10 AU yr^{-1} for low power requirements. Such speeds could enable spacecraft to travel out of the solar system within a 10-year mission. It has been speculated that this could be achieved by harnessing the solar wind dynamical pressure to thrust the spacecraft. Coupling to the solar wind would be produced through an artificial magnetosphere generated around the spacecraft either by utilizing a large-scale superconducting vacuum magnetic field or by injecting plasma into a magnetic field supported by solenoid coils on the spacecraft. Such an artificial magnetosphere has been proposed to work as a sail in the solar wind. The large spatial scales are required, since the dynamical pressure of the solar wind is much weaker than the radiation pressure of the Sun.

This report addresses both the plasma-free and plasma-inflated magnetospheric propulsion concepts called Plasma-Free Magnetospheric Propulsion (PFMP) and Mini-Magnetospheric Plasma Propulsion (M2P2). Deriving the scaling laws of the key parameters of these magnetospheric propulsion concepts, it can be shown that the plasma-free concept is theoretically sound, and force required to attain the expected speeds during an acceleration period of about 3 months is, in principle, possible to generate. In the case of the plasma-inflated concept, the injected plasma, however, introduces a third massive body in the system that introduces an additional sink for the solar wind momentum. Based on the scaling laws derived in the present study the force on the spacecraft due to the magnetopause current is much weaker than the momentum extracted from the solar wind. An obvious sink of momentum is the leakage of the plasma out from the magnetosphere. A possible way to retain significant acceleration would be that a current system to transfer the force acting on the magnetopause to the spacecraft is established very close to the spacecraft. However, it is beyond the present understanding of the problem, if the establishment of such a current system is physically feasible. Thus the plasma-inflated magnetosphere can be much less effective than the plasma-free magnetosphere for a given size of the magnetosphere.

To obtain a more quantitative picture of the propulsion concept, estimates for parameter ranges and requirements for computer simulations of both PFMP and M2P2 concepts are studied. This is done for a full-scale mission, and space-based and ground-based demonstrations of the propulsion concepts. For completeness, three methods of generating the magnetic field are studied: superconducting coil, ohmic coil, and a permanent magnet. We also consider two options of the space environment where the space-based demonstration could be done. One is on a low-altitude ionospheric orbit, and the other is an Earth-orbiting spacecraft in

the solar wind. The estimates for the computer memory and computing time requirements are obtained for MHD, hybrid, and full-particle simulations of the M2P2 concept.

The parameter ranges of the propulsion concepts are promising for a full-scale mission and space-based demonstrations: A force acting on the magnetopause adequate for desired levels of acceleration can be generated. However, the major issue in the case of M2P2 is the transfer of the magnetopause force to the spacecraft. The required current closure near the spacecraft implies that the plasma density has to be quite large. The existence of such a current system is presently an open question and can only be addressed by space-based or ground-based demonstrations or, perhaps, by computer simulations some day in the future.

On the ground, the demonstration has to be done in a vacuum chamber instead of a plasma chamber, in which the large magnetic field confining the plasma induces large forces on the current coil of the demonstrative apparatus. The parameter ranges show that the demonstration is feasible, at least for the PFMP concept using plasma velocities and densities of existing plasma guns. In the case of M2P2, the inflation of the magnetic field introduces additional complications in ground-based demonstrations.

The evaluation of computing requirements for MHD and hybrid simulations shows that a reasonable simulation approach is feasible. A pre-existing MHD simulation code used for planetary magnetospheres can be optimized for the parameter ranges of the magnetospheric propulsion concept in about three months assuming no unexpected complications would appear during the process. However, the large magnetic field magnitudes near the spacecraft increase the computing time significantly if the inner boundary of the simulation domain is considered at the spacecraft. In the case of hybrid simulation, the large magnetic field magnitudes may lead to considerable difficulties in adapting any pre-existing hybrid code to the issue of magnetospheric propulsion. At present, global full-particle simulations are far beyond the computing capacities.

From technological viewpoint the critical issue of a full-scale mission is related to the deployment of an artificial magnetosphere around the spacecraft. In the case of PFMP, the issue is the superconducting coil with large spatial scales (tens of kilometers), and for M2P2, the plasma source used for inflation of the artificial magnetosphere. Such a large-scale superconducting wire is beyond the present technology of superconducting materials for the characteristics required for the coil, passive cooling and operation closer to the Sun than 1 AU. On the other hand, there is a promising candidate for the plasma source of M2P2 based on a Rotating Magnetic Field (RMF) helicon.

For space-based demonstration, the most important issue is the measurement

of the acceleration of the demonstrative spacecraft. This can be done by using already available accelerometers, laser rangefinders, or methods based on the laser interferometry. Based on parameter ranges used in two laboratory experiments on the physics of the Earth's magnetosphere it is expected that laboratory experimenting on PFMP and M2P2 are technically feasible.

The demonstration mission is suggested to consist of a pair of spacecraft to be flown in the solar wind. One of the spacecraft is the primary spacecraft carrying the instruments to create the artificial magnetosphere, i.e., the magnetic coil and plasma source. As the demonstrative magnetosphere is smaller than that of the full-scale mission, both propulsion concepts can be addressed during a single mission. The second spacecraft is equipped to monitor the solar wind conditions, measure the acceleration of the spacecraft, and occasionally fly through the artificial magnetosphere to monitor its structure and plasma parameters. It is argued that the prototype qualitatively models the full-scale mission.

The prototyping of PFMP can be based on the pre-existing laboratory experiments, whereas in the case of M2P2, the inflation of the artificial magnetosphere complicates the experiment. It is suggested that the dynamic pressure of the simulated solar wind has to be gradually increased while the vacuum magnetic dipole is being inflated. Based on the earlier results on magnetospheric laboratory experiments, it can be argued that such experiments provide important information on the magnetospheric propulsion, especially in the case of M2P2: the electric currents flowing inside the magnetosphere can be studied in order to understand their role in transfering the solar wind pressure force on the magnetopause to the M2P2 spacecraft.

Regardless of its feasibility as a propulsive system a plasma-inflated magnetosphere may well have scientific and technical interest as a space-based demonstration for basic research in plasma physics and building plasma systems in space.

Contents

1 Introduction

1.1 The idea of magnetospheric propulsion

The idea of magnetospheric propulsion is to use the dynamic pressure (kinetic energy density) of the solar wind for spacecraft thrust. The idea is similar to that of a solar sail that harnesses the radiation pressure to push the spacecraft. In the case of magnetospheric propulsion, an obstacle to the solar wind flow, an artificial magnetosphere, is created around the spacecraft to absorb the momentum of the solar wind.

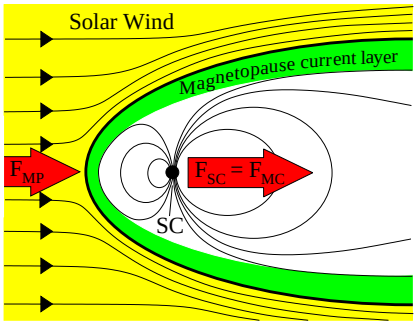

Figure 1: Schematics of an artificial magnetosphere.

The artificial magnetosphere is built by applying an internal strong magnetic field generated by electric coils attached to the spacecraft (Figure 1). The interaction between the internal magnetic field and the solar wind creates additional current systems. Most notably, a magnetopause current system, the so-called Chapman-Ferraro system is created to divert the solar wind around the artificial magnetosphere. However, as the solar wind dynamic pressure is much smaller than the radiation pressure, the spatial scales of the artificial magnetosphere have to be considerably larger than those of a solar sail. The required spatial scales have been proposed to be accomplished either (1) by elaborating a large vacuum magnetic field [*Zubrin,* 1993] or (2) by inflating further the magnetic field with plasma [*Winglee et al.,* 2000]. In this study these two magnetospheric propulsion systems are termed as Plasma-Free Magnetospheric Propulsion (PFMP) and Mini-Magnetospheric Plasma Propulsion (M2P2). It has been proposed that both PFMP and M2P2 can attain unprecedented speeds of about 50 km s^{-1} (10 AU yr^{-1}) with very low power requirements. In this study we consider the theoretical foundations, practical parameter ranges and technological feasibility for the PFMP and M2P2 systems.

1.2 Plasma-free Magnetospheric Propulsion (PFMP)

The basic concept of PFMP is to deploy a superconducting magnet in order to form an artificial magnetosphere around the spacecraft. The force acting on the spacecraft is given by the solar wind dynamic pressure multiplied by the cross-sectional area of the artificial magnetosphere. For a vacuum magnetic field (dipolar), the magnitude of the field falls off as r^{-3}. This implies that the magnetic moment of the magnetic coil on the spacecraft has to be substantially large to be able to push the magnetopause far enough from the spacecraft and to provide the magnetopause with a surface wide enough to gain adequate acceleration from the solar wind. In practice, this leads to large surface magnetic fields of the order a few Tesla and coil dimensions of tens of kilometres. Figure 2 shows a configuration proposed by *Zubrin* [1993].

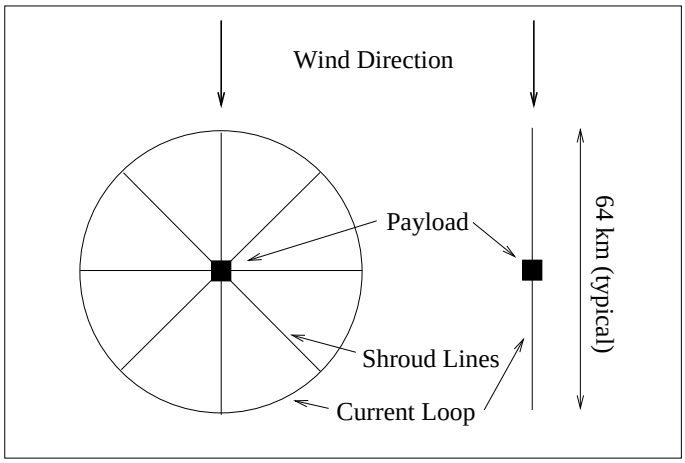

Figure 2: Configuration of the magnetic sail (after *Zubrin* [1993], the wind direction in the right configuration corrected).

1.3 Mini-Magnetosphere Plasma Propulsion (M2P2)

In PFMP the force acting on the spacecraft depends on the cross-sectional area of the artificial magnetosphere. Consequently, it was later suggested that by adding a plasma source to the spacecraft the magnetosphere would grow in size without increasing the dipole moment and thus a larger cross-sectional area would be reached [*Winglee et al.,* 2000].

In order to study such a system, *Winglee et al.* [2000] developed an MHD simulation from a pre-existing numerical simulation used for modeling the terrestrial magnetosphere [*Winglee et al.*, 1998a, b]. The approach was essentially based on

the Hall-MHD fluid equations. The large range of scale sizes (from 10 cm to 10 km) involved in the M2P2 concept was treated in the simulations by breaking the grid system up into a series (nine in all) of subsystems where the grid spacing increased by a factor of 2 between consecutive systems. Such a grid system allowed *Winglee et al.* [2000] to introduce a high spatial resolution around the spacecraft and resolve the reflection of the solar wind particles at the bow shock of the M2P2 magnetosphere. In absolute units, the largest subsystem represented 10 km, and the inner radius assumed a 10-m region around the spacecraft with a grid resolution of 2 m.

The inflation of the magnetosphere and steady state configuration for given solar wind parameters was obtained in a stepwise manner. Initially, a 1000-nT magnetic field was considered at the spacecraft. The simulation was then run for about four Alfvén wave transit times enabling an approximate equilibrium for the solar wind with a new configuration of M2P2. Once the equilibrium was established, the magnetic field strength was doubled, and the plasma injection was started allowing the solar wind interaction to find a new equilibrium. The process was repeated by increasing the magnetic field and the plasma density by factors of 2 and 4. The results of these runs suggested that the scale size of the M2P2 magnetosphere is directly proportional to the strength of the magnetic field. Extrapolating these results, *Winglee et al.* [2000] was able to obtain the magnitude of the magnetic field at the spacecraft (0.06 - 0.07 T) required for a subsolar distance of 15 km.

The simulation results showing the expanding magnetosphere were interpreted in terms of a heliospheric analogy. Due to the supersonically expanding solar wind and the rotation of the Sun the heliospheric magnetic field decays as r^{-1} in the solar equatorial plane and as r^{-2} in the direction of the poles, rather than r^{-3} as it is the case of a vacuum dipole or in the PFMP case. The decay rate smaller than that of r^{-3} is caused by the currents flowing inside the plasma. Such currents can flow only if there are substantial plasma pressure gradients or inertial forces to balance the Lorentz force (the $\mathbf{j} \times \mathbf{B}$ force) of the plasma currents. Figure 3 shows a schematic of the M2P2 system. In addition to the magnetopause currents, two other current systems based on the simulation results of *Winglee et al.* [2000] are sketched. One of the additional current systems is the tail current sheet, and the other is the system formed by a partial closure of the dayside magnetopause currents near the spacecraft via magnetic field-aligned currents.

In addition to the spacecraft and the solar wind, the injected plasma introduces a third massive body in the M2P2 system. Based on the results by *Winglee et al.* [2000], the injected plasma can escape from the M2P2 system at a rate of the order of 10^{-6} kg s^{-1}. If the escaping plasma is asymptotically accelerated to the solar wind speed, the momentum it extracts from the system is of the same order

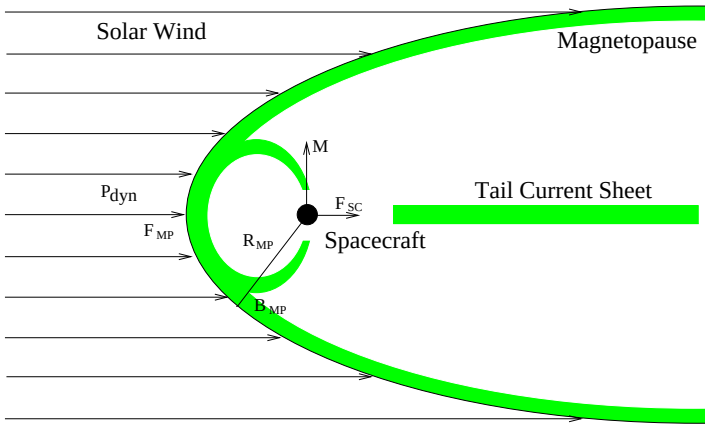

Figure 3: Schematics of the M2P2 system and its external current systems.

than the momentum of the solar wind at the magnetopause of M2P2.

One has also to be careful when estimating the decay of the magnetic flux density in the inflating plasma-filled magnetosphere. As shown in the text-books on solar wind expansion [*e.g., Priest*, 1982], the theoretically slowest possible decay ($\propto r^{-1}$) is obtained by the combined effect of expansion and rotation. The radial component decays as $B_r \propto r^{-2}$. However, as the magnetic field is frozen-in to the expanding plasma and the Sun rotates, the magnetic field in the equatorial plane is wound to form the famous Parker spiral. Consequently, the azimuthal component of the magnetic field scales as

$$B_\phi = \frac{v_\phi - r\Omega}{v_r} B_r \tag{1}$$

where Ω is the angular speed of solar rotation, v_r is the radial expansion speed and $v_\phi = \Omega R_\odot$ at the solar surface. From this eqation we see that the total equatorial field approaches the r^{-1}-dependence only at large r, i.e., when the spiral becomes tightly wound and the magnetic field is predominantly azimuthal.

1.4 Comparison of the key parameters of PFMP and M2P2

Table 1 shows a set of key parameters suggested for PFMP [*Zubrin,* 1993] and M2P2 [*Winglee et al.,* 2000]. While equal levels of acceleration are expected for both PFMP and M2P2, there are considerable differences in the parameters of these systems. These differences are basically caused by the spatial scale of the current coils on spacecraft being 31.6 km for PFMP and 10 cm for M2P2. This

evidently leads to vastly different masses of the coils. Thus based only on the numbers given, M2P2 is a far more advanced propulsion method than PFMP. The only feature in these numbers that favors PFMP is that the magnetic field magnitude at the spacecraft is clearly smaller for PFMP than for M2P2 (since the current coil of PFMP is further away from the spacecraft).

Key parameters	**PFMP**	**M2P2**
Subsolar point [km]	90	20
Coil diameter [km]	31.6	10^{-4}
Coil current [A]	50000	10
Coil mass [kg]	5000	10
Number of turns in the coil	1	1000
Magnetic moment of coil [A m^2]	$1.6{\cdot}10^{14}$	315
Coil surface magnetic field [T]	8	0.06
Magnetic field at spacecraft [T]	10^{-6}	0.06
Plasma density [cm^{-3}]	0	$5{\cdot}10^{13}$
Fuel consumption [kg day^{-1}]	0	0.5
Acceleration [m s^{-2}]	0.02	0.01

Table 1: Comparison of the parameters of PFMP and M2P2 as given by *Zubrin* [1993] and *Winglee et al.* [2000], respectively.

1.5 Technical issues

Technical problems will be discussed in Section 5. Here we list some main issues discussed by *Zubrin* [1993] and *Winglee et al.* [2000] to be kept in mind.

1.5.1 PFMP

Based on the key parameters of PFMP listed in Table 1, the major technical issue of PFMP is the large size of the superconducting coil. Any method of constructing such a coil in space is a nontrivial task, whether the coil was built on the ground and deployed in space or built in space. Once constructed, the magnetic tension maintains the shape of the coil in a form of a ring.

Another critical issue is the superconductivity of the coil. There is a critical current density that a given superconducting material can support. With low-temperature superconductors, a current density required by the PFMP concept can be achieved. The problem with the low-temperature superconductors is that the cooling of the coil has in practice to be passive (an active cooling system would be too expensive and heavy). Presently, the only way to introduce a

passive cooling of the coil is to coat it with multi-layer insulation and highly reflective coatings. The high temperature superconductors have demonstrated comparable critical currents at 77 K or more, but only in microscopic samples. Thus the temperature of the coil depends on the parameters of the material, and the superconducting state may not be accessible at 1 AU.

1.5.2 M2P2

While the spatial dimensions of the magnetic coil supporting the M2P2 system are reasonable, the inflation of the magnetic field introduces the major technological problem of M2P2: The inflating plasma has to be produced in presence of a strong magnetic field. Plasmas generated using electrodes cannot tolerate the high heat load at the high energy densities [*Winglee et al.,* 2000]. Thus presently there are few plasma sources that work in presence of strong magnetic field and even fewer capable of producing the high enough density required. However, inductive plasma sources such as helicons can produce the required level of density in presence of strong magnetic field [*Miljak and Chen*, 1998; *Gilliand et al.*, 1998]. Based on laboratory experiments, the inflation seems to occur in spatial dimensions of 0.4 m^{-3} and in time scales of the order of 1 s [*Winglee et al.*, 2001; *Ziemba et al.*, 2001].

The ultimate problem of M2P2 can also be the stability of the inflating plasma, since the plasma β (i.e., the ratio between the plasma and magnetic pressures) has to be large enough in order the plasma to change the magnetic field decay rate. Answers to the stability questions of the plasma expansion are not known. The stability issues may be quite different in space from those on the ground, and there were no resources to address these questions in detail in the present study

2 Theoretical discussion of magnetospheric propulsion systems

In this section, the theoretical background of PFMP and M2P2 is reviewed. An important part of this study is to identify the actual force acting upon the spacecraft. It is argued that the force is the Lorentz force acting on the internal coil of the spacecraft. The force is caused by the external electric currents in the artificial magnetosphere. Estimates for the force are derived both for PFMP and M2P2. In the case of PFMP, it is shown that the force acting on the magnetopause equals the Lorentz force of the magnetopause currents acting on the spacecraft.

In the case of PFMP, there are no other sinks of the solar wind momentum in the system. On the other hand, the plasma used to inflate the magnetosphere of M2P2 introduces an additional sink for the solar wind momentum, and the force acting on the magnetopause does not equal the force acting on the spacecraft. In the case of M2P2, additional external current systems are created. The contribution of these current systems is also taken into account when the total estimate of the Lorentz force is considered.

2.1 Identification of the force on the spacecraft

There are in principle two forces that can act on the spacecraft in electromagnetic systems such as PFMP and M2P2. One is caused by the plasma pressure gradients and the other by the electromagnetic interactions. The former can be disregarded, since it requires mechanical interaction between the plasma and the spacecraft, i.e., collisions of the plasma particles into the spacecraft. For the latter case, by definition, the magnetic force acting on the current coil of the spacecraft is the Lorentz force. The density of the Lorentz force can be expressed as $\mathbf{f}_{sc} = \mathbf{j}_{sc} \times \mathbf{B}_{ex}$. Here $\mathbf{j}_{sc}$ is the current density of the coil, and $\mathbf{B}_{ex}$ is the magnetic field caused by all external current systems that are induced by the solar wind interaction with the magnetic field of the coil of the spacecraft.

2.1.1 PFMP

With PFMP there are no conceptual problems. Solar wind momentum is transfered to the spacecraft, as the solar wind dynamic pressure excerts a certain force to the magnetopause surface, and this force must finally act on the spacecraft, since there is nothing else in the system that could be accelerated. Thus the magnetic field caused by the magnetopause currents transfers the solar wind momentum to the spacecraft through the Lorentz force.

2.1.2 M2P2

At first sight, the M2P2 idea also seems to follow sound physical principles: It rests on the same method of calculating the force as that applied in the case of PFMP. An MHD simulation of the system was constructed by *Winglee et al.* [2000]. These authors computed the force acting on the spacecraft by considering how much momentum is lost from the solar wind per unit time. Although this method is correct in the case of PFMP, it turns out to be incorrect in the case of M2P2. The reason is that in addition to the solar wind and the spacecraft, there

is a third massive body in the system, namely the plasma that has been injected from the spacecraft. The injected plasma will ultimately escape from the system and thus carry away momentum. Assuming that the plasma escapes at nearly the solar wind speed, the momentum loss can be expected to be significant.

2.2 Validity of the MHD approximation

In this study the MHD approximation is adopted to estimate the propulsive effects of PFMP and M2P2. The problem with MHD is that the size of the magnetosphere is small ($\sim$ 100 km) compared to the ion Larmor radius of solar wind particles. Thus, in principle, MHD is not valid at the magnetopause of the artificial magnetosphere and the MHD assumption may introduce unphysical results on the formation of the magnetopause. However, it is difficult to estimate the significance of the non-MHD effects to the propulsion.

2.2.1 PFMP

In the case of PFMP, non-MHD effects can be estimated, since all of the solar wind momentum lost in the interaction of the solar wind particles with the vacuum magnetic field is transferred to the spacecraft. According to the test particle simulations by *Zubrin* [1993], the force calculated as momentum loss of the test particle is of the same order as the force deduced from MHD force balance at the magnetopause.

2.2.2 M2P2

In the case of M2P2, the force acting on the spacecraft has to be computed as the Lorentz force induced by the external currents on the current coil internal to the spacecraft. It is obvious that the magnetopause currents are in reality distributed over larger spatial scales than in an idealistic MHD description, since the solar wind protons penetrate inside the MHD magnetopause. An estimate for the thickness of the magnetopause current layer can be given by tracing a test proton in a model representing the M2P2 magnetic field. Figure 4 shows a test particle trajectory of a solar wind proton with a velocity of 400 km/s. The spacecraft is located at the origin, and the proton was launched at the MHD magnetopause at X = 20 km and Y = 0 km. The proton penetrates at deepest to a radial distance of about 5 km from the spacecraft. Thus the magnetopause current can be expected to be distributed over a spatial range of about 15 km from the MHD magnetopause. This will evidently affect the MHD approach, but

we see no reason to expect that it would introduce deviations to the force larger than an order of magnitude from the real magnetopause current. On the other hand, inside the magnetosphere, the magnetic field increases, and at some radial distances from the spacecraft, the injected inflating plasma obeys very well the MHD equations. Finally, because the aim of this exercise is to derive scaling laws and order-of-magnitude estimates for various parameters of M2P2, we argue that the MHD approach is well suited for the study.

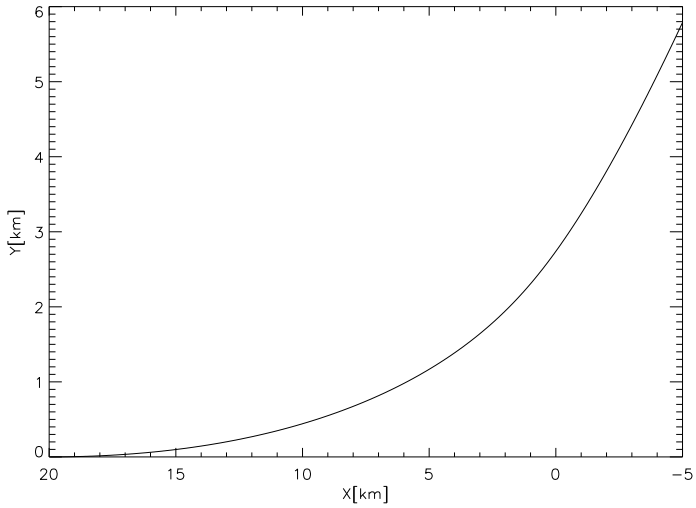

Figure 4: Trace of a solar wind proton in a magnetic field slope of r^{-1} with initial velocity of 400 km s^{-1}.

2.3 MHD scaling laws

In addition to the use of MHD, another approximation has to be made in order to derive the scaling law for the force acting on the spacecraft in the cases of PFMP and M2P2. One has to make a rough approximation for the gradient of the magnetic field at the spacecraft. This introduces the major simplification to the scaling laws derived in this work. Thus the details of the geometries of the current systems are not considered, and the numerical factors in the scaling laws correspond to simplified geometries. Most importantly, the scaling laws are intended to show the orders of magnitude of the key parameters, to provide us with estimates on the physical scales of the current coil at the spacecraft in the PFMP case, and to show that the M2P2 concept may provide much less thrust on the spaceraft than expected. However, any further refinement of these scaling laws is undermined by the fact that there is no full understanding of the solar wind plasma interaction with an artificial magnetosphere.

2.4 Estimation of acceleration in the plasma-free case

2.4.1 Force on the magnetopause

Consider a spacecraft with an artificial dipole moment M embedded in the solar wind whose dynamic pressure is $P_{\mathrm{dyn}} = \rho_{\mathrm{SW}} v_{\mathrm{SW}}^2$. Here ρ_{SW} and v_{SW} are the solar wind mass density (kg m^{-3}) and velocity (m/s). The dipolar magnetic field of the spacecraft is then

$$B(r) = \frac{\mu_0}{4\pi}\frac{M}{r^3}, \tag{2}$$

where r is the distance from the spacecraft. This equation is exactly valid only at the equatorial plane of the magnetosphere, but it allows us to compute the subsolar distance of the magnetopause, R_{MP}. This distance is determined from the MHD force balance condition

$$P_{\mathrm{dyn}} = \frac{B_{\mathrm{MP}}^2}{2\mu_0}, \tag{3}$$

where $B_{\mathrm{MP}} = B(R_{\mathrm{MP}})$ is the magnetic field just behind the magnetopause. We can neglect the interplanetary magnetic field, as the solar wind magnetic pressure is much smaller than the dynamic pressure. Together (2) and (3) imply

$$R_{\mathrm{MP}} = \left[\frac{\mu_0 M^2}{2(4\pi)^2 P_{\mathrm{dyn}}}\right]^{1/6}. \tag{4}$$

Assuming that the effective radius of the magnetosphere is equal to R_{MP} we obtain the force F that the solar wind exerts on the magnetopause as

$$F = P_{\mathrm{dyn}} \pi R_{\mathrm{MP}}^2. \tag{5}$$

Substituting the expression for R_{MP} from (4) into (5) we obtain

$$F = \pi^{1/3}\left(\frac{1}{16}\right)^{1/3} \mu_0^{1/3} P_{\mathrm{dyn}}^{2/3} M^{2/3}. \tag{6}$$

Inserting the numerical values of *Zubrin* [1993], we find $F = 283$ N, which is consistent with the results of *Zubrin* [1993].

2.4.2 Force on the spacecraft

In the case of PFMP, the force acting on the magnetopause has to be transferred completely to spacecraft, because there is nothing else in the system that could act as a sink of momentum, and thus the expression for the force (6) is also the correct

force acting on the spacecraft apart from a possible numerical factor of order unity. Such a factor may be related, for example, to the effective cross-sectional area of the magnetopause that is only approximately given by $\pi R_{\rm MP}^2$, to the approximative validity of MHD at the magnetopause, or to the fact that a small fraction of the solar wind plasma may leak in the vacuum PFMP magnetosphere. However, it is of interest to show that in the case of PFMP, the scaling laws of the forces on the magnetopause and spacecraft are equal.

Let us choose spacecraft-centered coordinates (x, y, z) so that the dipole moment is in the z-direction ($\mathbf{M} = M\hat{z}$), the solar wind flow is in the negative x-direction, and y completes the right-handed system. The only force that can act on the spacecraft is the Lorentz force, whose force density is $\mathbf{f} = \mathbf{j} \times \mathbf{B}$. Here $\mathbf{j}$ is the current density of the coil and $\mathbf{B}$ is the magnetic field caused by all magnetospheric current systems that develop, i.e. all magnetic fields excluding the field of the coil itself. (The force density of the field of the coil and the coil current density integrated in space gives zero net force.) Let us assume that the dipole moment is created by an ideal (singular) magnetic dipole, i.e. $\mathbf{j} = \nabla \times (\mathbf{M}\delta(\mathbf{x}))$ inside the spacecraft. Here $\delta(\mathbf{x})$ is the 3-D Dirac delta function. The total force on the spacecraft is the volume integral of the force density over all space,

$$\mathbf{F} = \int d^3\mathbf{x}\ \mathbf{j} \times \mathbf{B}. \tag{7}$$

Invoking the assumption that $\mathbf{M}$ is z-directed we see that $\mathbf{j}$ has only x- and y-components, and by symmetry the force $\mathbf{F}$ has only the x-component:

$$\begin{aligned} F_x &= \int d^3\mathbf{x} j_y B_z \\ &= -M_z \int d^3\mathbf{x} B_z \partial_x \delta(\mathbf{x}) \\ &= M_z \int d^3\mathbf{x} \delta(\mathbf{x}) \partial_x B_z \\ &= M_z \partial_x B_z. \end{aligned} \tag{8}$$

Here we only used the basic properties of the delta function. This result means that the force acting on the spacecraft is the dipole moment multiplied by the gradient of the magnetic field of all magnetospheric current systems, evaluated at the spacecraft location. The direction of the force is away from the Sun, i.e., F_x is negative, if $\partial_x B_z < 0$. Note that equation (8) is exact, involving no appriximations.

We cannot easily compute $\partial_x B_z$ analytically, but we can estimate its order of magnitude. Since this is the force acting on the spacecraft but it does not include any numerical factors arising from the actual geometry of the magnetopause, the estimates for other quantities in this work can rely on simplified geometries of the magnetopause and the current systems. The main contributor to B_z is

the Chapman-Ferraro current system, i.e. the magnetopause current sheet that separates the solar wind from the magnetosphere. This can be thought of as a large current sheet which is at the distance of $R_{\rm MP}$ away from the spacecraft. According to the force balance law (Eq. 3), the magnitude of the magnetic field created by the Chapman-Ferraro current system is $B_{\rm MP}$. Since the current sheet is at distance $R_{\rm MP}$ away from the spacecraft and there are no other length scales in the system, the gradient $\partial_x B_z$ must be proportional to $B_{\rm MP}/R_{\rm MP}$, and thus the force must be

$$\begin{aligned} F_x &\sim \frac{M B_{\rm MP}}{R_{\rm MP}} \\ &\sim \mu_0^{1/3} M^{2/3} P_{\rm dyn}^{2/3} \end{aligned} \tag{9}$$

where we used (3) and (4) and left out all numerical coefficients.

We see that the result (9) is, apart from numerical factors, identical with (6) derived in the previous subsection. Thus we have shown that in the plasma-free magnetosphere, the force acting on the spacecraft can be calculated in two methods A and B: In method A, we computed the force acting on the magnetopause and concluded that as there are no momentum sinks in the system, this force must be identical to the force acting on the spacecraft. In method B, we estimated the Lorentz force acting on the spacecraft more directly. Method B is not as useful for actual computation as method A because the numerical factors remain unknown, but serves to illustrate how the Lorentz force is the agent that transforms the force acting on the magnetopause to become the force acting on the spacecraft in the plasma-free case.

2.4.3 Acceleration of the spacecraft

Now assuming that the dipole moment is generated by a current loop with radius R and current I, the dipole moment is $M = I\pi R^2$, and we obtain from Eq. (6)

$$F = \pi \left(\frac{\mu_0}{16}\right)^{1/3} P_{\rm dyn}^{2/3} I^{2/3} R^{4/3}. \tag{10}$$

To compute the acceleration $a = F/m$ of the spacecraft we must know its mass m. Let us assume that the current-carrying wire has radius r and mass density ρ. Then the mass of the wire is

$$m_{\rm wire} = 2\pi R \pi r^2 \rho. \tag{11}$$

Let us further assume that the mass of the wire forms a fraction b of the total spacecraft mass ($0 < b < 1$, but due to the large size of the coil is b ~ 1), so that the total mass is

$$m = \frac{m_{\rm wire}}{b} = \frac{1}{b} 2\pi^2 R r^2 \rho, \tag{12}$$

and let us also express the current I flowing in the wire as $I = j\pi r^2$, where j is the current density in the wire ($\mathrm{A/m^2}$).

Putting everything together we obtain for the spacecraft acceleration

$$a = \frac{b}{\rho}\left[\frac{\mu_0}{128\pi}\frac{P_{\mathrm{dyn}}^2 j^2 R}{r^2}\right]^{1/3}. \tag{13}$$

For the numerical values used by *Zubrin* [1993], an acceleration of 0.09 $\mathrm{ms^{-2}}$ is achieved.

2.5 Estimation of acceleration in the M2P2 case

2.5.1 Force on the magnetopause

The scaling law for the force acting on the M2P2 magnetopause can be derived as the force on the PFMP magnetopause. In this case we must, however, take into account the slower radial decay of the M2P2 magnetic field. In order to do this, we assume a general radial dependence of the magnetic field as

$$B_r = B_0\left(\frac{L}{r}\right)^p, \tag{14}$$

where p defines the decay rate of the magnetic field at a distance r from the spacecraft, and L is the scale size of the spacecraft. Physically, $p > 1$. The surface field B_0 at the spacecraft can be expressed as

$$B_0 = \frac{\mu_o M}{4\pi L^3}. \tag{15}$$

In particular at the magnetopause, (14) reads as

$$B_{MP} = B_0\left(\frac{L}{R_{MP}}\right)^p. \tag{16}$$

Using the force balance (3) and (16), R_{MP} can be written as

$$R_{MP} = \frac{L B_0^{\frac{1}{p}}}{(2\mu_o P_{dyn})^{\frac{1}{2p}}}. \tag{17}$$

Using (15) and (16) the magnetic field magnitude at the magnetopause can be given in terms of R_{MP} as

$$B_{MP} = \pi^{-\frac{p}{3}} 2^{-\frac{2p}{3}} \mu_o^{\frac{p}{3}} M^{\frac{p}{3}} B_0^{1-\frac{p}{3}} R_{MP}^{-p}. \tag{18}$$

Expressing L in terms of the surface field B_0 (using L instead of B_0 would lead to a somewhat simpler expression for the force), we get

$$R_{MP} = \pi^{-\frac{1}{3}} 2^{-\frac{1}{2p}-\frac{2}{3}} \mu_o^{\frac{1}{3}-\frac{1}{2p}} M^{\frac{1}{3}} B_0^{\frac{1}{p}-\frac{1}{3}} P_{dyn}^{-\frac{1}{2p}}. \tag{19}$$

Using (5), the force on the magnetopause can be written as

$$F_{MP} = \pi^{\frac{1}{3}} 2^{-\frac{1}{p}-\frac{4}{3}} \mu_o^{\frac{2}{3}-\frac{1}{p}} M^{\frac{2}{3}} B_0^{\frac{2}{p}-\frac{2}{3}} P_{dyn}^{1-\frac{1}{p}}. \tag{20}$$

Note that choosing $p = 3$, (20) is identical to (6). Inserting the numerical values of $P_{dyn} = 2$ nPa, $B_0 = 0.01$ T, and $M = 314$ Am^2, F_{MP} equals to 2.7 N under the assumption of $p = 1$.

2.5.2 Force on the spacecraft due to the magnetopause current

As the magnetosphere of M2P2 is filled with plasma, (20) is not the force acting on the spacecraft. The force on the spacecraft due to the magnetopause currents has to be computed as

$$F_{SC} = \frac{M B_{\mathrm{MP}}}{R_{\mathrm{MP}}} \tag{21}$$

according to (9), i.e., the force that the external magnetic field causes on the magnetic coil attached to the spacecraft. Using expressions (18) and (19) to replace B_{MP} and R_{MP}, F_{SC} can be written as

$$F_{SC} = \pi^{\frac{1}{3}} 2^{\frac{1}{2p}+\frac{7}{6}} \mu_o^{\frac{1}{2p}+\frac{1}{6}} M^{\frac{2}{3}} B_0^{\frac{1}{3}-\frac{1}{p}} P_{dyn}^{\frac{1}{2}+\frac{1}{2p}}. \tag{22}$$

Inserting the numerical values used in (20), $F_{SC} = 2 \cdot 10^{-10}$ N.

The fact that the force acting on the spacecraft (23) is different (in fact, vastly different) from the force acting on the spacecraft (20) for $p \neq 3$ was not considered by *Winglee et al.* [2000] when postprocessing their MHD simulation results. The ratio of these two forces can be written as

$$\frac{F_{SC}}{F_{MP}} = 2^{\frac{3}{2p}+\frac{15}{6}} \mu_o^{\frac{3}{2p}-\frac{1}{2}} B_0^{1-\frac{3}{p}} P_{dyn}^{\frac{3}{2p}-\frac{1}{2}}. \tag{23}$$

Using the numerical values as $F_{MP} = 2.7$ N and $F_{MP} = 10^{-10}$ N, the force ratio equals to $8 \cdot 10^{-11}$, that is, of the order of 10^{-10}.

2.5.3 Magnetopause currents

In order to motivate physically that the force acting on the magnetopause is not equal to the force that acts on the spacecraft, we apply method B, i.e. estimate the

Lorentz force acting on the spacecraft directly. We use the expression $F = M\partial_x B_z$ where B_z is the magnetic field created by magnetospheric current systems. If we assume that the Chapman-Ferraro current system is the one that dominates in $\partial_x B_z$, the magnitude of $\partial_x B_z$ is *lower* than in the plasma-free case, because B_z is not modified, but the current sheet is farther away from the spacecraft, i.e. R_{MP} increases. This means that trying to inflate the mini-magnetosphere with plasma actually *reduces* the force acting on the spacecraft, because it makes the magnetic field due to magnetospheric current systems vary less steeply at the point where the spacecraft is located. Using (9) and numercal values of P_{dyn} = 2 nPa and M = 314 A m^2, we find the force F = $2{\cdot}10^{-10}$ N that is orders of magnitude smaller than the force exerted on the magnetopause.

The most critical hypothesis in the order of magnitude estimates above is that $\partial_x B_z \propto B_{\mathrm{MP}}/R_{\mathrm{MP}}$, i.e., there are no other critical length scales in the current system generated by the solar wind interaction with the inflated magnetosphere. This aspect is further studied below.

2.5.4 Currents inside the M2P2 magnetosphere

In the case of M2P2, currents can also flow in the plasma used for inflating the internal magnetic field of the spacecraft. This occurs if the plasma gradients are large enough to support them. According to the simulation results of *Winglee et al.* [2000] such internal current systems are formed and they are qualitatively similar to those of the Earth's magnetosphere, including, for example, the cross-tail current sheet. More importantly, the magnetopause currents are partially closed near the spacecraft via field-aligned currents in the dayside. Similar behaviour of the Chapman-Ferraro currents is also known to occur in the Earth's magnetosphere [*e.g., Janhunen and Koskinen*, 1997]. This current system is important since it provides M2P2 with currents that could flow near the spacecraft and could, in principle, be able to enhance the magnetic field gradient at the satellite location. However, based on the contribution of the magnetopause currents to the force acting on the spacraft we expect that the currents inside the magnetosphere have to flow really close to the spacecraft in order to significantly enhance the force acting on the spacecraft. In the case of the Earth, the ionospheric currents cause a force on the Earth's dipole that is of the same order (10^7 N) as the force acting on the magnetopause (See section 2.7). Thus the ionospheric currents contribute to the transfer of the magnetopause force to the Earth. Note, however, that the terrestrial magnetosphere is much closer to a PFMP than an M2P2 system since the magnetosphere is practically a vacuum as compared to the solar wind. Thus the dayside magnetic field decays as r^{-3} (except just below the magnetopause current layer).

In order to estimate the effects of possible currents closing near the spacecraft, we calculate the ratio between the forces F_{MP} and F_{CC} caused by the magnetopause and closure currents, respectively. Figure 5 shows a schematic presentation of the day-side partial closure of the magnetopause currents.

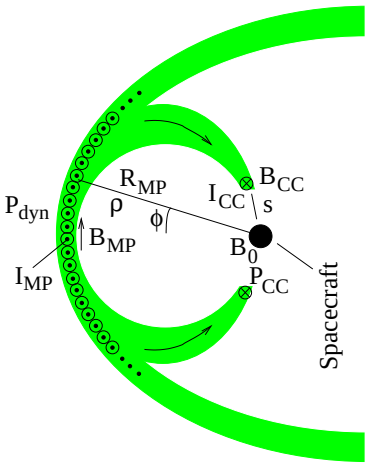

Figure 5: Geometry of the closure current partially closing the magnetopause current near the spacecraft.

An estimate for F_{MP} was already given in section 2.5.1, where it was the same as the force on the spacecraft F_{SC}. In order to estimate F_{CC}, the magnetopause is assumed to be cylindrically symmetric in such a way that the symmetry axis (z′ coordinate) is parallel to the magnetopause current at the subsolar point (Figure 5). In such a geometry, the MHD force balance equation can be written in cylindrical coordinates as

$$\partial_\rho P = j_{z'} B_\phi. \tag{24}$$

If the magnetopause is considered as infinitely thin, the pressure can be expressed as $P = P_{dyn}\theta(\rho - R_{MP})$ in terms of the step function θ. Integrating (24) over the magnetopause as

$$\int_{MP} \partial_\rho (P_{dyn}\theta(\rho - R_{MP}))\rho d\rho d\phi = \int_{MP} j_z B_{MP} da, \tag{25}$$

noting that $\partial_\rho \theta(\rho - R_{MP}) = \delta(\rho - R_{MP})$, and assuming that the magnetic field is constant at the magnetopause, we get

$$\pi P_{dyn} R_{MP} = I_{MP} B_{MP}\,. \tag{26}$$

Assuming that a fraction α of the total day-side current I_{MP} is diverted to close near the spacecraft, the closure current can be written as

$$I_{CC} = \alpha I_{MP} = \frac{\pi \alpha P_{dyn} R_{MP}}{B_{MP}}. \tag{27}$$

The magnetic field caused by I_{CC} both on the northern and southern hemispheres can be calculated from the Biot - Savart law

$$B_{CC} = \frac{\mu_o I_{CC}}{\pi s}, \tag{28}$$

where s is the distance of I_{CC} from the spacecraft. Following equation (8), the force F_{CC} can be calculated as

$$\begin{aligned} F_{CC} &= M_z \partial_x B_z = M_z \frac{B_{CC}}{s} \\ &= M_z \frac{\mu_o I_{CC}}{\pi s^2} = M_z \frac{\mu_o \alpha P_{dyn} R_{MP}}{B_{MP} s^2}. \end{aligned} \tag{29}$$

The fraction of the two forces is then

$$\begin{aligned} \frac{F_{CC}}{F_{SC}} &= \frac{\mu_o \alpha P_{dyn} R_{MP}}{2 B_{MP} s^2} \frac{R_{\mathrm{MP}}}{B_{\mathrm{MP}}} \\ &= \frac{\alpha}{2} \left(\frac{R_{MP}}{s} \right)^2, \end{aligned} \tag{30}$$

and the distance s of the closure current from the spacecraft for a given fraction is

$$s = R_{MP} \left(\frac{\alpha}{2} \frac{F_{SC}}{F_{CC}} \right)^{\frac{1}{2}}. \tag{31}$$

Considering that $F_{SC} = 8 \cdot 10^{-11} \cdot F_{MP}$, the condition $F_{CC} \approx F_{MP}$ requires that the currents have to close really close to the spacecraft. Assuming that $\alpha = 0.1$ and $R_{MP} = 20$ km, the currents have to close 4 cm away from the spacecraft. Even at the unphysical limit of all magnetopause current closing near the spacecraft, i.e., $\alpha = 1$, they would have to close 13 cm away from the spacecraft.

Furthermore, we want to estimate the plasma pressure and density required in the vicinity of the spacecraft to support the current I_{CC}. Assuming that the pressure gradients and current density have spatial scales of s and s^2, respectively, the force balance ($\nabla P = \mathbf{j} \times \mathbf{B}$) can be written as

$$\frac{P_{CC}}{s} = \frac{I_{CC}}{s^2} B_s, \tag{32}$$

where B_s is the magnetic field magnitude at the distance of s from the spacecraft. Using (27) and the scaling law (14), P_{CC} can be written as

$$P_{CC} = \frac{\pi \alpha P_{dyn} R_{MP}}{B_{MP} s} \left(\frac{L}{s} \right)^p B_0, \tag{33}$$

where L is the scale size of the spacecraft, and B_0 is the internal magnetic field at the spacecraft. Applying (14) to rewrite B_{MP}, the ratio between P_{CC} and P_{dyn} can be expressed as

$$\frac{P_{CC}}{P_{dyn}} = \pi\alpha \left(\frac{R_{MP}}{s}\right) \left(\frac{L}{R_{MP}}\right)^{-p} \left(\frac{L}{s}\right)^{p} = \pi\alpha \left(\frac{R_{MP}}{s}\right)^{1+p}. \tag{34}$$

With $p = 1$, $\alpha = 0.1$, $R_{MP} = 20$ km, $s = 4$ cm, and $P_{dyn} = 2$ nPa, the plasma pressure 4 cm away from the spacecraft is 157 Pa. Assuming thermal equilibrium ($P_{CC} = n_s kT$), the density n_s reads as

$$n_s = \pi\alpha \frac{P_{dyn}}{kT} \left(\frac{R_{MP}}{s}\right)^{1+p}, \tag{35}$$

where T is the temperature of the inflating plasma, and k is the Boltzmann constant. For a given temperature of 4 eV [*Winglee et al.,* 2000], plasma density near the spacecraft is 10^{20} m^{-3}.

Production and maintenance of such a high-density plasma environment around the spacecraft may lead to severe complications in practice. In principle, there are two possible ways to try to avoid such high densities. One is to increase the plasma temperature, and the other is to use a technological system to close the current. However, the temperature of 4 eV corresponds to a temperature of over 40000 K, which would lead large heat fluxes near the spacecraft. Thus the latter alternative may be the only way to avoid the large densities near the spacecraft. However, we do not know of any realistic ideas how to build a system to capture the current.

2.5.5 Acceleration of the spacecraft

The fact that only a small fraction of the force affecting on the magnetopause is transferred to act on the spacecraft as the Lorentz force was apparently overlooked by *Winglee et al.* [2000]. They computed the force acting on the magnetopause (by several different methods all producing equivalent results) and assumed that the same force must also act on the spacecraft, because that is the case in the plasma-free case. The latter assumption, which is never explicitly mentioned in their paper but is made implicitly, is simply not true when there is escaping plasma present in the system. Our argumentation above shows that the presence of the plasma tends to make the force acting on the spacecraft smaller, not to increase it, even though the momentum transferred from the solar wind increases. However, it is impossible in the current state of analysis to provide an accurate quantitative estimate of this effect.

2.6 Open vs. closed field lines

The escape of the injected plasma from the M2P2 system takes place effectively only along open magnetic field lines. Thus one could argue that if most of the magnetic field lines of the M2P2 system are closed, the plasma escape is negligible, and the spacecraft is pushed by the magnetopause force (6). However, it can be shown by geometrical arguments that the slower than r^{-3} spatial decay of the magnetic field in the M2P2 system implies that a significant portion of the magnetic field lines must be open (recall that the r^{-2} field of an electric point charge is fully open and the same would apply to a magnetic monopole).

Let the magnetic field be expressed in terms of the Euler potentials α and β as

$$\mathbf{B} = \nabla\alpha \times \nabla\beta. \tag{36}$$

This presentation is convenient, since α and β are constant along the magnetic field lines, or in other words, the magnetic field lines are equicontours of α and β. For simplicity, we consider the magnetic field in the midnight meridional plane of the M2P2 system: For symmetry reasons, the magnetic field has no component normal to this plane. We choose spherical coordinates in such a way that the unit vectors $\mathbf{e}_\rho$ and $\mathbf{e}_\theta$ are in the plane, and $\mathbf{e}_\phi$ is normal to the plane. Thus ϕ is constant in this plane and can be chosen as β. In general, if

$$\alpha = f(\theta)r^k, \tag{37}$$

the radial dependence of $\mathbf{B}$ is r^{k-2}. The criterion for closed field lines is $k < 0$, i.e., $p > 2$, which follows from (37): α must go to zero when r approaches to infinity. This can be motivated by plotting the equicontours of α. Figure 6 shows these equicontours for $f(\theta) = \sin(\theta)$ and $k = -1$(a :p = 3), $k = -0.5$(b :p = 2.5), and $k = 0$(c :p = 2). The magnetic field lines for different k show that when k approaches zero the field lines become open.

Note that this argumentation is not in contradiction with the fact that locally the dayside magnetospheres of, e.g., the Earth and Mercury are compressed and thus their radial decay in the equatorial plane behind the dayside magnetopause is slower than r^{-3}. This compression does not affect on the amount of open flux in the polar regions, and in fact is opposite to the idea of inflation by a plasma source.

In principle, the arguments presented here are local, and it could be argued that the field lines may close at distances larger than those considered here. This would need a current system additional to the magnetopause current system in the far tail of the artificial magnetosphere. However, based on our knowledge on the Earth's magnetosphere, there is no such current system, and a large fraction of the magnetic flux of the polar regions is open to the solar wind through the

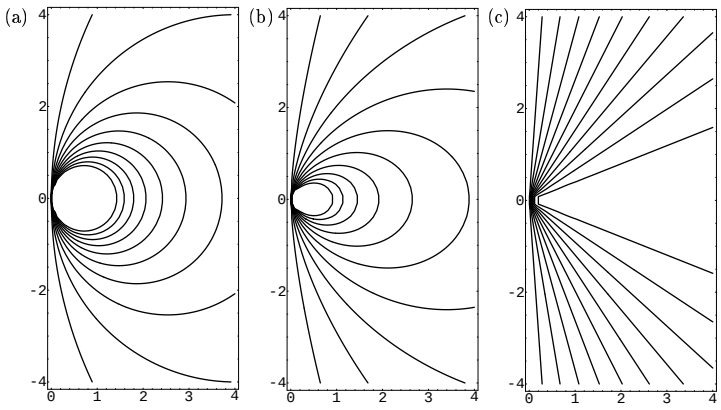

Figure 6: Equicontours of α or field lines of the corresponding magnetic field for three values of k: (a) $k = -1 (p = 3)$, (b) $k = -0.5 (p = 2.5)$, and (c) $k = 0 (p = 2)$

tail lobes. Similarly, in the case of the Sun all plasma eventually escapes from the heliosphere.

2.7 Application to the Earth

The Earth's magnetosphere provides us with an example of magnetospheric propulsion in nature. In practice, the magnetosphere is a vacuum relative to the solar wind and can be considered as a PFMP type of a system: the major current system is the Chapman-Ferraro system. However, there are external currents flowing also inside the terrestrial magnetosphere, and a fraction of these currents closes in the ionosphere. This notion allows us to look at the transfer of the magnetopause force to the Earth.

According to (5), the force on the magnetopause was given as

$$F = P_{\mathrm{dyn}} \pi R_{\mathrm{MP}}^2.$$

The sub-solar point of the Earth's magnetopause (R_{MP}) is typically 12 R_E which corresponds to a force (F) of $3.7{\cdot}10^7$ N for a typical solar wind dynamical pressure P_{dyn} of 2 nPa. As the force is perpendicular to the motion of the Earth, it does not perform work. The only effect is an insignificant decrease of the gravitational force of the Sun that is $3.6{\cdot}10^{22}$ N.

As discussed in (4.2.2.), the currents (I_{CC}) closing in the ionosphere cause a magnetic perturbation (B_{CC})

$$B_{CC} = \frac{\mu_o I_{CC} \sin \lambda}{\pi s}$$

at a distance s from the current system. The latitudinal term $\sin\lambda$ has been added here, as the ionospheric currents flow in the polar region of the Earth. Using (8), the force generated by the ionospheric current systems to act on the Earth's dipole field can be estimated as

$$\begin{aligned} F_{CC} &= M_z \frac{B_{CC}}{s} \\ &= M_z \frac{\mu_o I_{CC} \sin\lambda}{\pi s^2}. \end{aligned}$$

The magnetic moment of the Earth is $8.05{\cdot}10^{22}$ Am^2, s can be taken to be 1 R_E, and I_{CC} is typically 50 kA. For these numerical values and $\lambda = 20°$, F_{CC} equals to $1.4{\cdot}10^7$ N that is of the same order as the force acting on the magnetopause. Thus the ionospheric closure currents contribute to the force transfer.

Note that in the terrestrial magnetosphere the currents between the magnetopause and ionosphere flow for the most part in a very good ideal MHD plasma, whereas they close in the resistive non-MHD ionosphere. This is rather different from the M2P2, and no direct conclusions concerning the closure currents in M2P2 should be made from our knowledge of this system.

From the terrestrial magnetosphere, the mass outflow is about 2 kgs^{-1}. This mass flow is picked up by the solar wind and accelerated to the speed of the solar wind. For a typical solar wind speed of 400 kms^{-1}, the acceleration corresponds to a force of $8{\cdot}10^5$ N that is two orders of magnitude less than the force acting on the Earth.

3 Investigation of relevant parameters for demonstration purposes

In this section we discuss the ranges of the important parameters for magnetospheric propulsion based on the scaling laws derived above. First we rewrite the scaling laws for the M2P2 concept in terms of the spatial scale L of the spacecraft, or more generally the size of the dipolar region around the spacecraft. In this form the scaling law for the force acting on the M2P2 magnetopause reads as

$$F_{\mathrm{MP}} = \pi^{1-\frac{2}{p}} 2^{-\frac{5}{p}} \mu_o^{\frac{1}{p}} M^{\frac{2}{p}} L^{2-\frac{6}{p}} P_d^{1-\frac{1}{p}}. \tag{38}$$

The force on the spacecraft due to the magnetopause currents reads as

$$F_{\mathrm{SC}} = \pi^{\frac{1}{p}} 2^{\frac{5}{2p}+\frac{1}{2}} \mu_o^{-\frac{1}{2p}+\frac{1}{2}} M^{1-\frac{1}{p}} L^{\frac{3}{p}-1} P_d^{\frac{1}{2}+\frac{1}{2p}}. \tag{39}$$

From this form, it is easy to see that at the limit of $p = 1$, the dipolar region is the effective cross-section of the artificial magnetosphere of M2P2 for the solar wind pressure. As it was shown in Section 2, the actual force acting on the spacecraft due to the magnetopause current is only $\sim 10^{-10}$ of the force acting on the magnetopause. The smallness of this factor makes it meaningless to base estimates of the parameter ranges of M2P2 on the scaling law (39). Thus it is obvious that the feasibility of the M2P2 concept relies on the currents that possibly close near the spacecraft and that estimates for such currents have to be found in addition to the straightforward estimates for the force acting on the magnetopause.

There are several methods of measuring the acceleration of the spacecraft in space-based demonstrations:

- Accelerometer on board the spacecraft
- Doppler radar
- Interferometry using two spacecraft

Sensitivity of the order of 10^{-9} ms^{-2} can be taken as a baseline acceleration level using accelerometers in the space-based demonstrations (http://www.onera.fr/dmph-en/accelerometre/index.html). Recently, the Doppler radar methods were used to measure the anomalous deceleration of Pioneer 10 and 11 to the level of 10^{-8} ms^{-2} [*Anderson et al.,* 2002]. The acceleration of 10^{-9} ms^{-2} corresponds to a displacement of about 4 m a day. Such a displacement can easily be measured using two spacecraft. Thus we consider here the acceleration levels larger than 10^{-9} ms^{-2} for the space-based demonstration.

3.1 PFMP full-scale mission

Feasibility of the PFMP concept as a propulsion system for a full-scale mission depends mostly on the size of the current loop used in generation of the vacuum artificial magnetosphere around the spacecraft. In order to achieve the desired speed of about 50 km s^{-1}, an acceleration of about 0.01 m s^{-2} has to be generated by the magnetospheric propulsion. For typical solar wind conditions, it can be shown that the size of the loop is basically defined by the current density in the current loop. Figure 7 shows the radius of the current loop as a function of the current density for ten levels of acceleration (Coil Radius vs. Current Density plot, CRCD plot). It can be seen that reduction of the radius of the current loop from that given by *Zubrin* [1993] (30 km) requires superconductors that can handle current densities larger than 10^{10} A m^{-2}. A current density of 10^{11} A m^{-2}

would provide the spacecraft with an acceleration of 0.01 m s^{-2}, with a radius of the current loop of 3 km.

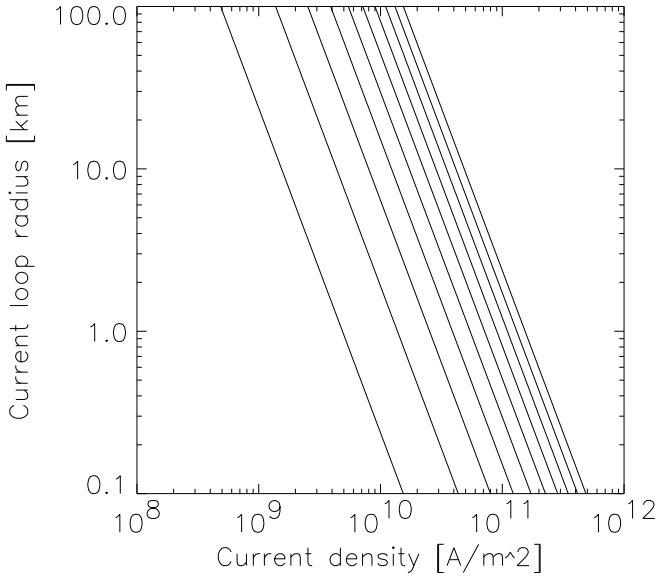

Figure 7: CRCD plot (the radius of the current loop as a function of the current density) for PFMP full-scale mission for ten levels of accelerations (from left to right 0.001 to 0.01 m s^{-2}, spaced by 0.001 m s^{-2}). Other parameter values read as $b = 0.75$, $P_{\mathrm{dyn}} = 2$ nPa, and $r = 1$ mm.

3.2 PFMP space-based demonstration in the ionosphere

In principle, demonstrations of the magnetospheric propulsion concepts can also be considered in the ionosphere. A dynamic pressure needed for demonstration of the propulsion effects can be estimated: On an orbit at an altitude of about 800 km, the spacecraft speed is about 7.5 km s^{-1} and number density about 10^5 cm^{-3}, which gives dynamic pressure with respect to the spacecraft frame of reference of about 10 nPa. However, at this altitude the Earth's magnetic field is about $4{\cdot}10^{-5}$ T (at the poles). This corresponds to a magnetic pressure of 0.6 mPa implying that the dynamic pressure can be neglected for the estimation of the size of the artificial magnetosphere. Thus the size of the magnetosphere has

to be given as

$$R_{\mathrm{mp}} = \left(\frac{\mu_o M}{4\pi B_{\oplus}} \right)^{\frac{1}{3}}, \tag{40}$$

where $B_{\oplus}$ is the magnitude of the Earth's magnetic field at about 800 km. The acceleration can then be given as

$$a = \frac{b}{\rho} \left[\frac{\mu_0^2}{2\pi N_l} \frac{j^2 R}{r^2 B_{\oplus}^2} \right]^{1/3} P_d, \tag{41}$$

where N_l is the number of turns in the current coil. Furthermore, the magnetic force on the magnetic field of the spacecraft caused by the Earth's magnetic field has to be taken into account when measurements on propulsive effects are processed. At low altitudes, the mass density of the neutral atoms exceeds the mass density of the plasma. Thus if the artificial magnetosphere is not large enough, the spacecraft drag due to the dynamic pressure of the neutrals can exceed the drag caused by the plasma.

As a minor point, it can also be pointed out that the interaction between the ionospheric plasma and the artificial magnetosphere would be subalfvénic. If these shortcomings can be accepted, a low-altitude demonstration would provide us with a low-cost space-based demonstration of the magnetospheric propulsion effects. Demonstrations of the propulsive effects of PFMP in the ionosphere can be based on a magnetic field generated by a superconducting coil, traditional ohmic coil, or a permanent magnet. An additional motivation for such a system is that it could potentially be applied for studies of spacecraft re-entry to the atmosphere.

3.2.1 Superconductor

In the case of a superconducting coil, Figure 7 is replotted for lower acceleration levels as Figure 8. When flying in the ionosphere, the superconducting state of the current coil has to be actively maintained. This assumes a cooling system that has to be taken into account in the estimates of the total mass of the demonstrative spacecraft. Here, we include this fact in the parameter b that gives the ratio of the current coil to the total mass of the spacecraft. We assume here that $b = 0.05$.

3.2.2 Ohmic conductor

Considering a traditional ohmic conductor, the current density has to be reduced by several orders of magnitude compared to the case of a superconducting coil.

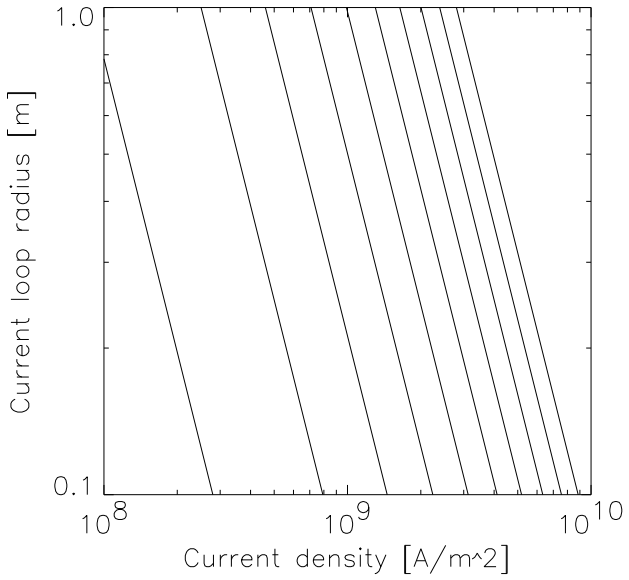

Figure 8: CRCD plot for an ionospheric demonstration of PFMP using superconductor: ten levels of accelerations (from left to right 10^{-7} to 10^{-6}, spaced by 10^{-7} m s^{-2}). Other parameter values read as $b = 0.05$, $P_{\rm dyn} = 10$ nPa, $r = 1$ mm., and $N_c = 1$.

The current density can be expressed in terms of the Ohmic power density p_Ω in the wire as

$$j = \sqrt{\frac{p_\Omega}{r_\Omega}}, \tag{42}$$

where r_Ω is the resistivity of the current wire. The Ohmic power density sets up the upper limit for the current density in the current coil and depends on the characteristics of the coil material. For copper, a current density of 1 A mm^{-2} corresponds to about 150 kW m^{-3}. In order to generate a magnetic field large enough to push the magnetopause outside the spacecraft, the coil has to have several turns for low current densities. Figure 9 shows several levels of acceleration gained by the spacecraft using an Ohmic coil. Figure 9 has the same format as Figures 7 and 8. The range of the current density (from 10^6 to 10^8 A m^{-2}) is based on the numbers given above. Furthermore, the scale size is reduced to the range from 0.1 to 1 m. Note, the largest current densities plotted correspond to a large Ohmic heating in the current coil.

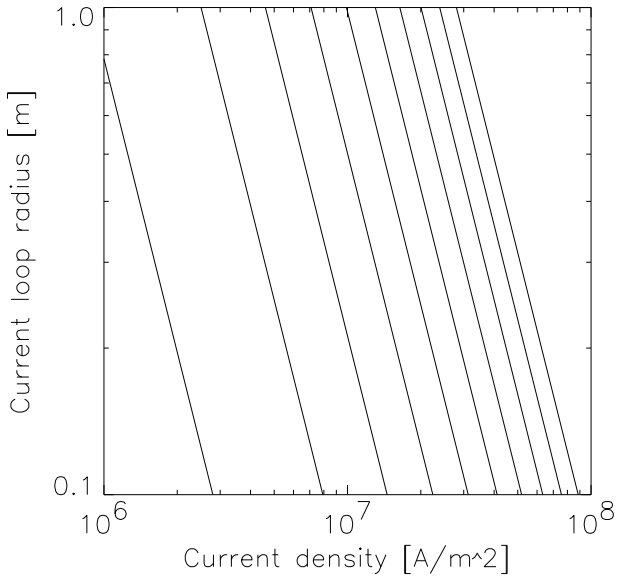

Figure 9: CRCD plot for an ionospheric demonstration of PFMP using ohmic conductor: ten levels of accelerations (from left to right 10^{-8} to 10^{-7}, spaced by 10^{-8} m s^{-2}). Other parameter values read as $b = 0.5$, $P_{\rm dyn} = 10$ nPa, $r = 1$ mm., and $N_c = 100$.

3.2.3 Permanent magnet

Estimates for a cylindrical permanent magnet can be deduced from the equation

$$B_{\rm pm} = \frac{B_{ri}}{2}\left(\frac{h}{\sqrt{R_2^2+h^2}} - \frac{h}{\sqrt{R_1^2+h^2}}\right), \tag{43}$$

where B_d is the magnetic field at the symmetry axis of the magnet at the top of the magnet, B_{ri} is the residual induction, R_2 is the outer radius of the ring, R_1 is the inner radius of the ring, and h is the length of the magnet (http://www.magnetsales.com/Design/DesignG.htm). The mass of such a magnet is given by

$$m_{\rm pm} = \pi\rho_{\rm pm}h(R_2^2 - R_1^2), \tag{44}$$

where $\rho_{\rm pm}$ is the density of the magnetic material. Expressing R_1 as $R_1 = \xi R_2$ ($\xi < 1$) in terms of R_2, the acceleration can written as

$$a = \left(\frac{B_{\rm pm}}{B_\oplus}\right)^{\frac{2}{3}} \frac{P_d}{\rho_{\rm pm}h(1-\xi^2)} \tag{45}$$

Figure 10 shows several different levels of acceleration of a demonstrative spacecraft as functions of the residual induction and mass density of the magnet. The spatial scales of the magnet are scaled as $h = 1$ cm, $R_2 = 10$ cm, and $R_1 = 9$ cm.

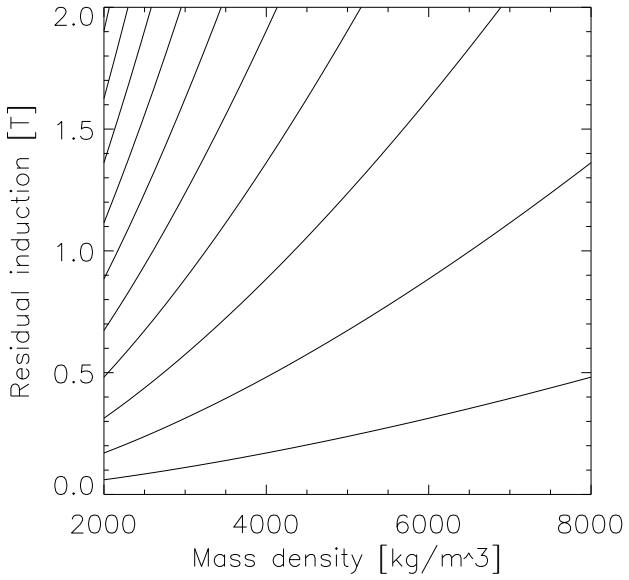

Figure 10: Ionospheric demonstration of PFMP using permanent magnet. The residual induction of the magnetic material as a function of the mass density of the material for ten levels of accelerations (from bottom to top, 10^{-9} to 10^{-8} ms^{-2}, spaced by 10^{-9} m s^{-2}). The dynamical pressure $P_{\rm dyn} = 10$ nPa.

3.3 PFMP space-spaced demonstration in the solar wind

In the solar wind the dynamical pressure is typically 2 nPa, but it may easily be of the same order than in the case of the ionospheric demonstration (10 nPa). However, in the solar wind the magnetic field can be neglected in the determination of the size of the artificial magnetosphere. This leads to parameter ranges different from those derived for an ionospheric demonstration.

3.3.1 Superconductor

Figure 11 shows a CRCD plot for ten levels of acceleration. Using superconductor, a small scale size for the coil attached to the spacecraft can be obtained with

acceleration ranging from 10^{-5} to 10^{-4} m s^{-2}.

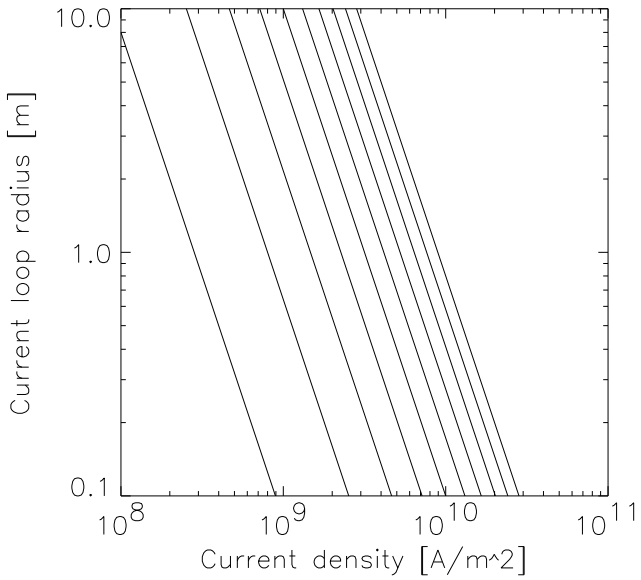

Figure 11: CRCD plot for a solar-wind demonstration of PFMP using superconductor: ten levels of accelerations (from left to right 10^{-5} to 10^{-4}, spaced by 10^{-5} m s^{-2}). Other parameter values read as $b = 0.5$, $P_{\rm dyn} = 2$ nPa, $r = 1$ mm.

3.3.2 Ohmic conductor

Figure 12 shows a CRCD plot for ten levels of acceleration in the case of an Ohmic conductor. The scale size similar to that of a superconducting system provides the spacecraft with only an acceleration level of 10^{-7} to 10^{-6} m s^{-2}, which is two orders of magnitude less than that provided by the superconducting coil.

3.3.3 Permanent magnet

Figure 13 shows the residual induction of the magnetic material as a function of the mass density. The scale sizes of the permanent magnet read as $h = 1$ cm, $R_2 = 10$ cm, and $R_1 = 9$ cm (see section 3.2.3 for the magnet design). Acceleration levels similar to those gained by the Ohmic coil can be obtained also by using a permanent magnet.

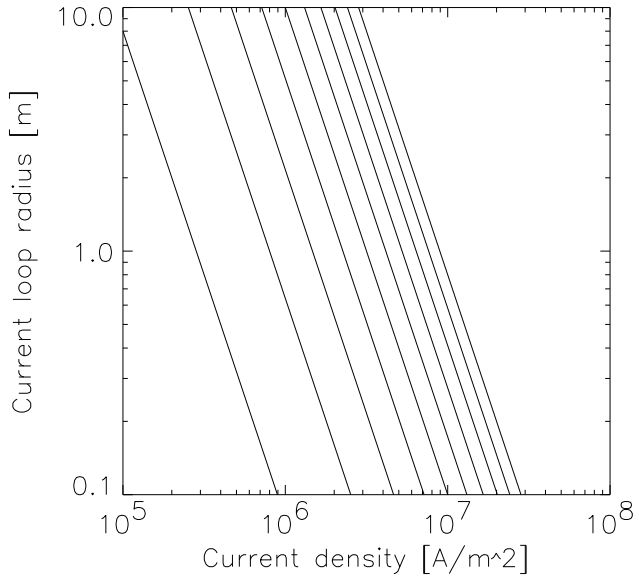

Figure 12: CRCD plot for a solar-wind demonstration of PFMP using ohmic conductor: ten levels of acceleration (from left to right 10^{-7} to 10^{-6}, spaced by 10^{-7} m s^{-2}). Other parameter values read as $b = 0.5$, $P_{\rm dyn} = 2$ nPa, $r = 1$ mm.

3.4 M2P2 full-scale and space-based demonstration in the solar wind

For M2P2 the magnetic field attached to the spacecraft can easily be created by any of the methods considered above, and it is unnecessary to consider here all the options for the generation of the magnetic field. Instead, the main issue here is the transfer of the force acting on the magnetopause to the spacecraft. According to the scaling laws derived in Section 2, the desired level of acceleration can only be achieved by the M2P2 concept if a considerable fraction of the external currents of the M2P2 magnetosphere closes in the vicinity of the spacecraft.

Figure 14 shows the plasma number density as a function of the distance from the spacecraft for several levels of acceleration (see figure caption for the values). The solid (dashed) lines correspond to the magnetic field decay power of 1 (2). The triangles show the required distance from the spacecraft for the magnetopause currents to partially close, so that they fully transfer the force acting on the magnetopause to the spacecraft. The currents have to close at the distance of about 6 cm from the spacecraft in the case of $p = 1$. In the case of $p = 2$, this

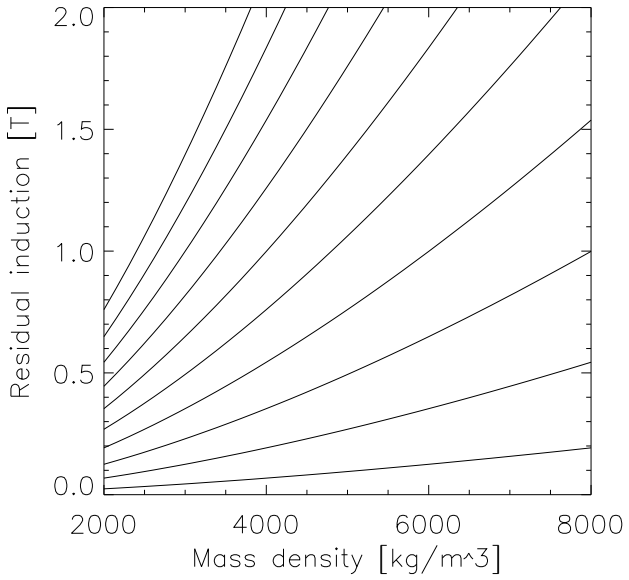

Figure 13: The residual induction of the magnetic material as a function of the mass density of the material for ten levels of acceleration (from bottom to top, 10^{-7} to 10^{-6} m s^{-2}, spaced by 10^{-7} m s^{-2}). The dynamical pressure, $P_{\rm dyn} = 2$ nPa.

distance depends on the desired level of acceleration and varies between 70 cm and 20 m. For a full-scale mission, the plasma density has to be between the orders of 10^{19} m^{-3} ($p = 1$) and 10^{17} m^{-3} ($p = 2$) for the required acceleration of 0.01 m s^{-2}. For space-based demonstration purposes, a plasma density from about 10^{15} m^{-3} ($p = 1$) to about 10^{14} m^{-3} ($p = 2$) is required for an acceleration of about 10^{-6} m s^{-2}. Note that the acceleration level of $p = 2$ implies larger magnetic moment at the spacecraft.

Based on a recent study by *Slough and Miller* [2000] plasma densities given in Figure 14 can be produced by presently available plasma sources.

There are several aspects to be taken into account when the feasibility of the maximum of the plasma densities of Figure 14 is considered: recombination, heat flux, total mass of the injected plasma, and technical aspects related to the plasma source. The total mass of the injected plasma sets no limitation to the plasma density. However, if the electrons of the injected plasma mechanically interact with the spacecraft, a large heat flux from the plasma can be expected. The heat flux can be estimated as nv_ekT with electron number density (n), velocity (v_e),

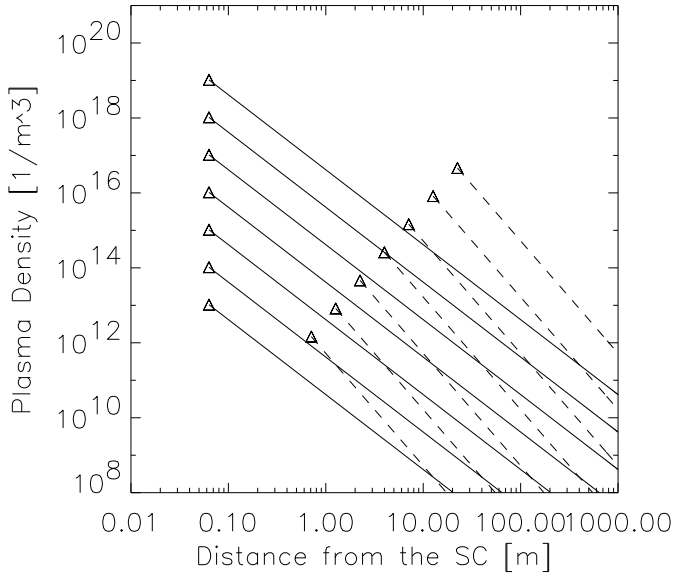

Figure 14: M2P2 full-scale mission and space-based demonstration in the solar wind: Plasma number density as a function of the distance from the spacecraft for seven levels of acceleration for magnetic field decay power p of 1 (solid lines) and 2 (dashed lines) (from bottom to top, 10^{-8}, 10^{-7}, 10^{-6}, 10^{-5}, 10^{-4}, 10^{-3}, 10^{-2} m s^{-2}). The dynamical pressure is 2 nPa, the mass of the spacecraft is 100 kg, and $\alpha = 0.1$. The triangles indicate the the distance at which the magnetopause force is fully transferred to the spacecraft.

and temperature (T). For the density (10^{19} m^{-3}) and temperature of the given plasma (4 eV), the heat flux is about 10^8 W m^{-2}, which the spacecraft cannot tolerate. Note that the heat flux cannot be reduced by using a colder plasma due to recombination. Thus the plasma densities given in Figure 14 are feasible only if the spacecraft can be insulated from the plasma. Note that the insulation cannot be provided by the magnetic field. As the plasma is collisional, the loss cone is full and the particles hit the spacecraft surface.

If a magnetic field decay power larger than 1 is assumed, the magnetic moment required at the spacecraft increases considerably from the values adequate in the case of $p = 1$. Figure 15 shows the acceleration of the spacecraft as functions of the magnetic field decay power p and magnetic moment M for the same levels of acceleration as in Figure 14. Note that Figure 15 assumes that closure currents have both to exist and close at the distances indicated by triangles in Figure 14. It can be seen that for a full-scale mission, the magnetic moment has to be

between the orders of 100 A m^2 ($p = 1$) and 10^7 A m^2 ($p = 2$) for the required acceleration of 0.01 m s^{-2}. For space-based demonstration purposes, a magnetic moment from about 1 A m^2 ($p = 1$) to about 10^3 A m^2 ($p = 2$) is required for an acceleration of about 10^{-6} m s^{-2}.

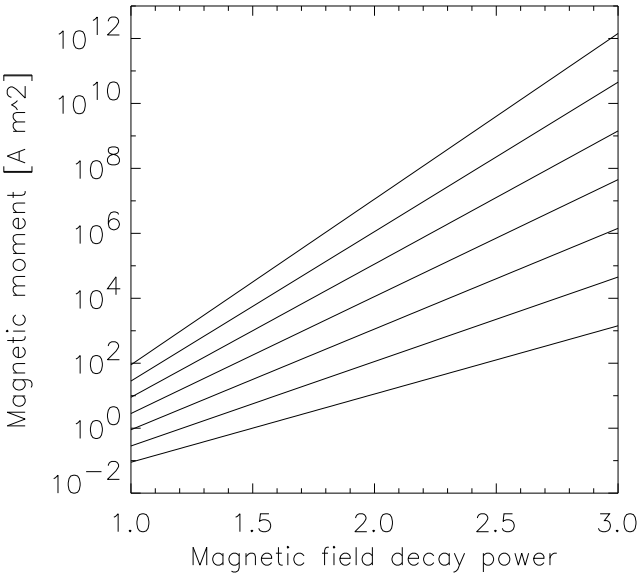

Figure 15: M2P2 full-scale mission and space-based demonstration in the solar wind: Magnetic moment as a function of the magnetic field decay power for several levels of acceleration (from bottom to top, 10^{-8}, 10^{-7}, 10^{-6}, 10^{-5}, 10^{-4}, 10^{-3}, 10^{-2} m s^{-2}), if closure currents exist and close at the distances as shown in Figure 14. The dynamical pressure is 2 nPa, the mass of the spacecraft is 100 kg, and $\alpha = 0.1$.

In order to complete the parametric study of the M2P2 propulsion concept it is important to look at the ratio between the forces generated by the closure currents to affect the spacecraft (F_{CC}) and the solar wind to affect the magnetopause (F_{MP}) as a function of the distance from the spacecraft. Using the corresponding scaling laws of (6) and (38), this ratio ϵ can be written as

$$\epsilon = \alpha 2^{\frac{5}{2p}-\frac{1}{2}} \pi^{\frac{1}{3}-\frac{1}{p}} \mu_o^{\frac{1}{2}-\frac{1}{2p}} P_d^{\frac{1}{2p}-\frac{1}{2}} M^{1-\frac{1}{p}} L^{\frac{3}{p}-1} s^{-2}. \tag{46}$$

Figure 16 shows ϵ in the cases of $p = 1$ (solid line) and $p = 2$ (dashed lines) for the density profiles of Figure 14, i.e., the maxima of ϵ correspond to the triangles shown in Figure 14. It can be seen that ϵ is decreased by a factor of 10^{-4}, if the distance of the current closure is increased by a factor of 100. In the case of

$p = 2$ the same ϵ can be reached with larger distance of the closure region if the magnetic moment at the spacecraft was increased.

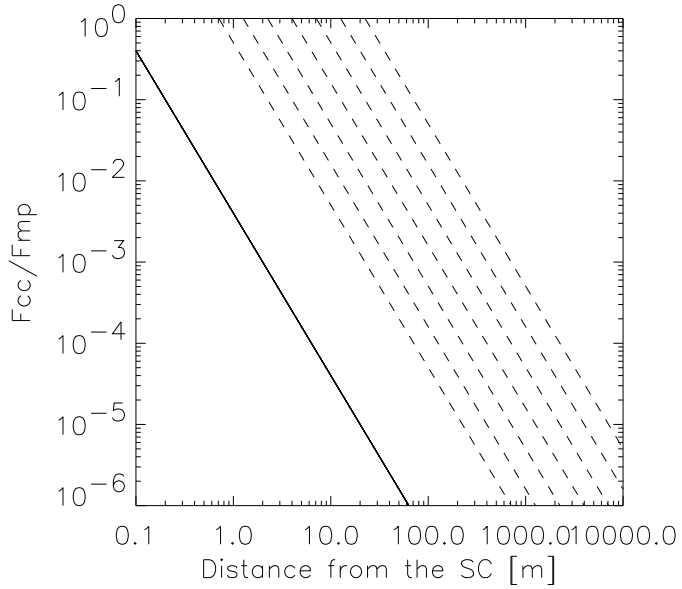

Figure 16: M2P2 full-scale mission and space-based demonstration in the solar wind: Ratio between the forces generated by the closure currents to the spacecraft (F_{CC}) and the solar wind to the magnetopause (F_{MP}) as a function of distance from the spacecraft. Both, the case of $p = 1$ (solid line) and $p = 2$ (dashed lines) corresponding to the profiles of Figure 14 are shown. The maximum ratios are achieved by the distances marked by the triangles in Figure 14.

The parametric study here shows that M2P2 can reach the acceleration level of 10^{-6} m s^{-2} with a reasonable plasma density near the spacecraft, if the magnetopause currents are closed close enough to the spacecraft. This can be studied by a space-based demonstration. For a full-scale mission (acceleration level of 10^{-2} m s^{-2}), the currents have to close through a high-density plasma in the vicinity of the spacecraft in order to transfer the solar wind momentum to the spacecraft. This is very critical since the efficiency of the force transfer falls drastically with increasing current closure distance from the spacecraft (Figure 16). However, these critical aspects may possibly be avoided, if the magnetic moment at the spacecraft is increased and the magnetic field decays as r^{-2} ($p = 2$), which would imply both lower plasma density and more distant current closure from the spacecraft than in the case of $p = 1$.

3.5 M2P2 space-based demonstration in the ionosphere

Here we seek for parameter ranges that provide the spacecraft with such an acceleration that can be measured, if the force acting on the spacecraft is effectively enough transferred to the spacecraft. Since the plasma density of M2P2 is high compared to the neutral density at the altitude of 800 km, the interaction between the plasma and the atmospheric neutral atoms has to be taken into account, when the measurements of the propulsive effects are processed. Figure 17 shows the plasma density as a function of the current closure distance from the spacecraft. The force on the magnetopause is transferred to the spacecraft, if the current closure region is at a distance of about 1 m away from the spacecraft. This requires a plasma density of 10^{11} to 10^{14} m^{-3} for acceleration levels of 10^{-8} to 10^{-5} m s^{-2}.

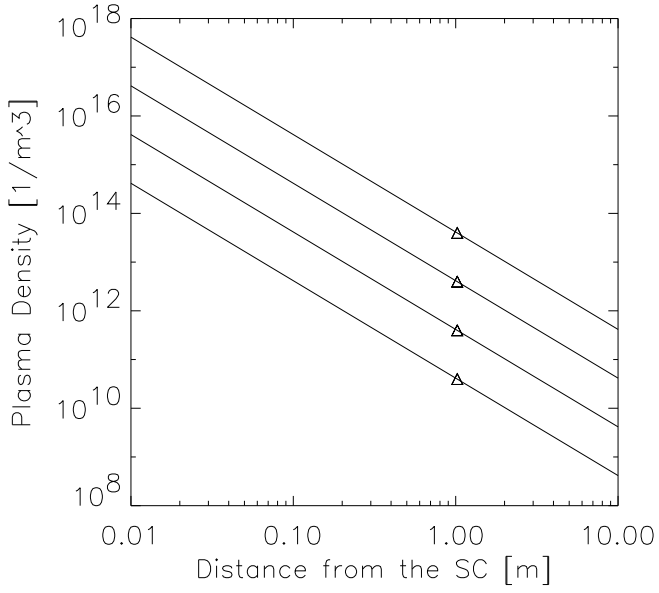

Figure 17: M2P2 space-based demonstration in the ionosphere: Plasma number density as a function of the distance from the spacecraft for seven levels of acceleration (from bottom to top, 10^{-8}, 10^{-7}, 10^{-6}, 10^{-5} m s^{-2}). The mass of the spacecraft is 100 kg, and $\alpha = 0.1$.

3.6 Ground-based demonstration

3.6.1 PFMP

In order to demonstrate the propulsive effects of PFMP and M2P2 in a plasma chamber the parameters for space-based demonstration in the ionosphere (Figure 8) indicate that with a coil of 10 cm in radius and 10^7 A m^{-2} of current density an acceleration of about 10^{-8} m s^{-2} can be achieved. In the ionosphere, the dynamic pressure was typically 10 nPa (800-km orbit). This pressure corresponds to a spacecraft speed of 7.5 km s^{-1}.

Whether such plasma flow speeds are feasible for the present plasma chambers, will be discussed in Section 5.2.4. The plasma flow can also be based on an ion beam in a vacuum chamber. Such a demonstration would allow us to neglect the magnetic forces induced to the current coil by the magnetic fields confining the plasma in the plasma chamber.

Here we consider the dynamical pressure of 10 nPa. Such a pressure can be obtained by varying the plasma flow speed and density in the plasma chamber. Figure 18 shows plasma density as a function of the plasma flow speed. It can be seen that the desired level of acceleration can be achieved even with low plasma flow speeds, if higher plasma densities than those in the ionosphere can be introduced in the plasma chamber.

3.6.2 M2P2

The parameter ranges of PFMP (section 3.6.1) can be adopted for the demonstration on the magnetopause force in the case of M2P2. Using a dynamical pressure of 10 nPa, a force of 10^{-8} N can be expected at the magnetopause of M2P2. In order to demonstrate the transfer of the magnetopause force to the demonstrative spacecraft, an estimate for the distance of the current closure and the plasma density at the current closure region has to be obtained. The numbers given here correspond to the values of $L = 5$ cm, and $R_{\mathrm{mp}} = 50$ cm. For these values, the current has to close about 3 cm from the demonstrative spacecraft. The plasma density in this region has to exceed $3{\cdot}10^{11}$ m^{-3} in order the plasma to be able to close the current.

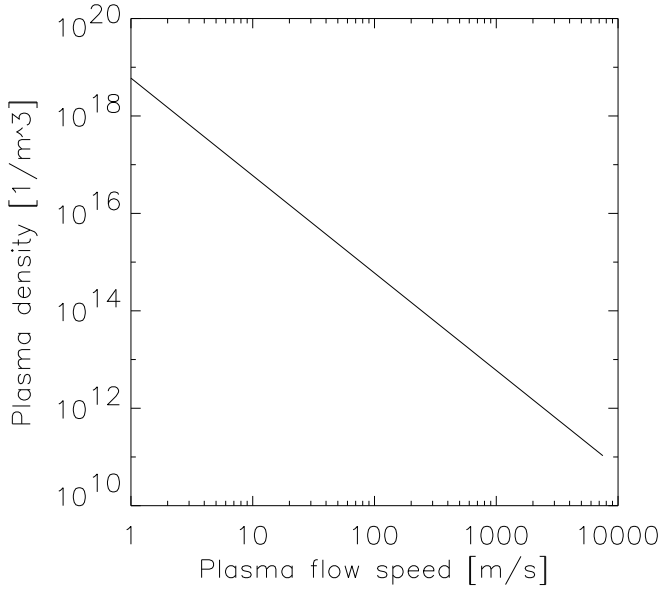

Figure 18: Ground-based demonstration of PFMP: Plasma number density as a function of the plasma flow speed. The curve corresponds to a dynamic pressure of 10 nPa and magnetopause force of 10^{-8} N.

4 Requirements for computer simulations

Based on the parameter ranges derived in the previous section the key physical points the computer simulation has to address are the formation of the magnetopause, generation of the magnetopause currents, and partial closure of these currents near the spacecraft. Especially, the closure currents are problematic in a sense that they connect two regions of vastly different physical parameters, high-magnetic field region near the spacecraft to a non-MHD region near the magnetopause. The connection between the near-spacecraft region and the magnetopause also complicates any efforts of separate simulations for the magnetopause formation and the near-spacecraft regions. Whether a simulation can produce the physical key features, remains uncertain until actual simulations have been made. Given the limited resources available for this project, unfortunately, no final answer to this question can be given here. Nevertheless, the computing requirements are thoroughly analysed in the following and could be used as guidelines for possible extension of the present study.

4.1 Applicability of simulation approaches

There are basically three simulation approaches to the plasma physics relevant to the magnetospheric propulsion: MHD simulation, hybrid simulation, or full-particle simulation. Applicability of these simulation schemes depends on the plasma parameters characterizing the system to be simulated.

Considering the MHD approach, it was shown in Section 2 that the Larmor radius of a solar wind proton in the M2P2 magnetosphere is about 15 km, i.e., of the same order as the spatial scale size of the M2P2 magnetosphere. Thus the MHD approach is invalid in most parts of the M2P2 magnetosphere. However, the MHD description of the Earth's magnetosphere is also, in principle, invalid, but as it reproduces well the large-scale features of the Earth's magnetosphere, the MHD approach can be considered to be a useful simulation approach to the physics of the M2P2 magnetosphere. It is also important to note that the studies on the boundary layers of the Earth's magnetosphere indicate that the magnetopause is thicker than the Larmor radius of a solar wind proton. This implies that a magnetopause boundary layer may cover the entire M2P2 magnetosphere. In other words, the magnetopause currents are distributed over a spatial range significantly larger than that given by the MHD approximation, which describes the magnetopause as a discontinuity separating the magnetosphere and the solar wind. This affects on both the possible closure of the magnetopause currents near the spacecraft and the transfer of the solar wind momentum to the spacecraft.

In a hybrid simulation, the finite thickness of the magnetopause boundary layer is better described, since the ions are considered as particles in the simulation. Thus more realistic simulation of the physics of the M2P2 magnetosphere can be expected by using the hybrid approach. The main problem concerning the applicability of the hybrid approach is the fact that the equations for hybrid simulation cannot be written in a conservative form. This results in numerical instabilities in the simulation that typically lead to unlimited growth of energy, especially the magnetic energy.

The full-particle simulation approach would give a complete description of the M2P2 physics. However, as shown below, a global full-particle simulation is far beyond the present computer capacity and can be disregarded as a realistic approach to the M2P2 physics. Regardless of this fact, the full-particle simulations can be locally applied to some M2P2 issues such as magnetopause formation, thickness, and structure, but possibly also to the interactions of the injected plasma near the spacecraft.

4.2 Model for estimation of computing requirements

In this section, estimates for computing requirements are presented for MHD, hybrid, and full particle simulations. In order to do this, we define a set of equations that models the system to be simulated as

$$
\begin{aligned}
B(r) &= B_L \left(\frac{L}{r}\right)^p && (47)\\
B_L &= \frac{\mu_0 M}{4\pi L^3} && (48)\\
n(r) &= n_L \left(\frac{L}{r}\right)^2 && (49)\\
B(r_{mp}) &= \sqrt{\mu_0 P_d} && (50)\\
n(r_{mp}) &= n_{sw}. && (51)
\end{aligned}
$$

These equations are: Radial dependence (r) of the magnetic field magnitude ($B(r)$); Boundary condition for the magnetic field magnitude, the magnetic field magnitude ($B_L = B(L)$) at the spacecraft (L); Radial dependence of the plasma number density ($n(r)$); Boundary condition at the outer boundary of the simulation box, the magnetic field magnitude ($B(r_{mp})$) at the magnetopause (r_{mp}); and Boundary condition for the plasma density at the magnetopause, the solar wind plasma density n_{sw}. In addition to the listed variables, the set of equations includes the dynamic pressure of the solar wind P_d, the magnetic moment of the current coil attached to the spacecraft M, and the ion mass used in the simulation m_i. The radial dependence of the magnetic field can alternatively be given as

$$B(r) = B_{mp} \left(\frac{r_{mp}}{r}\right)^p. \quad (52)$$

The density profile can also be written as

$$n(r) = n_{mp} \left(\frac{r_{mp}}{r}\right)^2. \quad (53)$$

In order to estimate the computing time, we introduce a dimensionless factor N_{sw} that is the number of times it takes for the solar wind to flow across the length scale of the artificial magnetosphere during a simulation run time. In terms of N_{sw}, the physical time to be simulated can be written as

$$T = N_{sw} \frac{R_{\mathrm{MP}}}{V_{sw}}, \quad (54)$$

where R_{MP} is the spatial scale size of the system, the distance to the magnetopause. In other words, as R_{MP}/V_{sw} is the time it takes for the solar wind to

pass once the length scale of the artificial magnetosphere ($R_{\rm MP}$), the total physical simulation time is then N_{sw} times the single passage. In general, the number of cells N_c in the given model can be found by integrating over the system spatial scales as

$$N_c = \int_{r_s}^{r_{mp}} dN_c = \int_{r_s}^{r_{mp}} \frac{4\pi r^2 dr}{\Delta X^3}, \tag{55}$$

where ΔX^3 is the volume of a single grid. The total number of propagated cells corresponding to a desired physical time period of T to be simulated is given as

$$N = \int_{r_s}^{r_{mp}} dN_c \int_0^T \frac{dt}{\Delta t} = \int_{r_s}^{r_{mp}} \frac{4\pi r^2 dr}{\Delta X^3} \frac{dt}{\Delta t}. \tag{56}$$

Finally, let N_{comp} be the number of cells the computer calculates in second, and the computer time can be given as

$$T_{comp}[s] = \frac{N}{N_{comp}} \tag{57}$$

4.3 MHD

4.3.1 Number of cells and memory requirements

In MHD, an adaptive grid size can be taken to be

$$\Delta X = kr, \tag{58}$$

where k is constant, typically $k \simeq 0.1$. The number of cells N_c (55) in a simulation box is

$$N_c = \int_{r_s}^{r_{mp}} \frac{4\pi r^2 dr}{k^3 r^3} = \frac{4\pi}{k^3} \ln\left(\frac{r_{mp}}{r_s}\right). \tag{59}$$

For numerical values of $r_s = 10$ m, $k = 0.1$, $r_{\rm mp} = 30$ km, the number of cells is $N_c \approx 10^5$. Typically, an MHD simulation uses 800 bytes per cell, which gives an estimate of 80 MB of memory.

4.3.2 Time step and computing time

In an MHD simulation, the time step of the simulation is defined by the Alfvén velocity V_A and the grid size ΔX as

$$\Delta t \leq C_{\rm CFL} \frac{\Delta X}{V_A}, \tag{60}$$

where C_{CFL} is constant and, typically, $C_{\mathrm{CFL}} \simeq 0.4$ (Courant condition). According to the model above, the Alfvén velocity is given as

$$V_A(r) = \frac{B(r)}{\sqrt{\mu_0 m_i n(r)}} \tag{61}$$

or alternatively as

$$V_A(r) = V_{sw}\left(\frac{r_{mp}}{r}\right)^{p-1} \tag{62}$$

In the case of an adaptive time step, N can be computed as

$$N = \int_{r_s}^{r_{mp}} \frac{4\pi r^2}{k^3 r^3} dr \int_0^T \frac{V_A}{C_{\mathrm{CFL}} k r} dt. \tag{63}$$

Using (62) and executing the integrals this can be written as

$$N = \frac{4\pi T V_{sw}}{k^4 C_{\mathrm{CFL}} p r_{mp}} \left[\left(\frac{r_{mp}}{r_s}\right)^p - 1\right] \approx \frac{4\pi T V_{sw}}{k^4 C_{\mathrm{CFL}} p r_{mp}} \left(\frac{r_{mp}}{r_s}\right)^p \tag{64}$$

Using (54), (64) reads as

$$N = \frac{4\pi N_{sw}}{k^4 C_{\mathrm{CFL}} p} \left(\frac{r_{mp}}{r_s}\right)^p \tag{65}$$

In (65), r_{mp}^p can be rewritten by using (47), (48), and (50) as $(L^{p-3} B_L)/\sqrt{\mu_o P_d}$, and (65) reads as

$$N = \frac{N_{sw} \mu_o^{\frac{1}{2}} M}{k^4 C_{\mathrm{CFL}} p L^3 P_d^{\frac{1}{2}}} \left(\frac{L}{r_s}\right)^p \tag{66}$$

The computer time is then given as

$$T_{comp} = \frac{N_{sw}}{k^4 N_{comp} C_{\mathrm{CFL}} p} \left(\frac{L}{r_s}\right)^p L^{-3} \mu_o^{\frac{1}{2}} M P_d^{-\frac{1}{2}}. \tag{67}$$

For numerical values of $p = 1$, $k = 0.1$, $N_{sw} = 10^4$, $N_{comp} = 10^6$, L=0.1 m, r_s = 10 m, M = 150 A m^2, P_d = 2nPa, the computing time $T_{comp} \approx 10$ days. Note that in order to study the current closure at the distance of 1 m ($r_s = 1$ m) with magnetic field decay power of $p = 1$ ($p = 2$), the computing time would increase to about 100 days (1000 days).

4.4 Hybrid simulation

4.4.1 Number of cells and memory requirements

In the case of a hybrid simulation, the grid size is defined here as the inertial length of the electrons as

$$\Delta X = l_{pe} = \frac{c}{\omega_{pe}}, \tag{68}$$

where c is the speed of light and ω_{pe} is the electron plasma frequency

$$\omega_{pe} = \sqrt{\frac{ne^2}{\epsilon_0 m_e}}. \tag{69}$$

The number of cells in the simulation can be calculated as

$$N_c = \int_{r_s}^{r_{mp}} \frac{4\pi r^2 dr}{\Delta X^3} = \frac{4\pi}{c^3} \int_{r_s}^{r_{mp}} \omega_{pi}^3 r^2 dr. \tag{70}$$

For convenience, it can be shown that

$$\omega_{pe} = \omega_{pe}^{sw} \left(\frac{r_{mp}}{r} \right). \tag{71}$$

The number of cells can then be written as

$$N_c = \frac{4\pi(\omega_{pe}^{sw})^3}{c^3} \int_{r_s}^{r_{mp}} \left(\frac{r_{mp}}{r} \right)^3 r^2 dr = 4\pi \left(\frac{r_{mp}}{l_{pe}^{sw}} \right)^3 \ln \left(\frac{r_{mp}}{r_s} \right). \tag{72}$$

For numerical values of $r_s = 10$ m, $l_{pe}^{sw} = 2$ km (assumes solar wind electron density of $6.5 \cdot 10^6$ m^{-3}), $r_{\mathrm{mp}} = 30$ km, the number of cells $N_c \approx 3 \cdot 10^5$. Typically, a hybrid simulation uses about 2000 bytes per cell, which gives an estimate of 600 MB of memory required.

4.4.2 Time step and computing time

The time step is given by the Courant condition as

$$\Delta t \leq C_{\mathrm{CFL}} \frac{\Delta X}{V_W}, \tag{73}$$

where V_W is the whistler velocity that can be approximated as

$$V_W \approx \sqrt{2} V_A. \tag{74}$$

The number of propagated cells in time T can be integrated by using (56) as

$$N = \int_{r_s}^{r_{mp}} \frac{4\pi r^2 dr}{l_{pe}^3} \int_0^T \frac{\sqrt{2} V_A}{C_{\mathrm{CFL}} l_{pe}} dt. \tag{75}$$

In a fashion similar to that of the derivation of N in the case of MHD, N can be written as

$$N = \frac{\sqrt{2} \cdot 4\pi N_{sw}}{p C_{\mathrm{CFL}}} \left(\frac{r_{mp}}{l_{pe}^{sw}} \right)^4 \left(\frac{r_{\mathrm{mp}}}{r_s} \right)^p, \tag{76}$$

where l_{pi}^{sw} is the ion inertial length at the magnetopause. The computer time can be expressed as

$$T_{comp} = \frac{\sqrt{2} \cdot (4\pi)^{-\frac{4}{p}} N_{sw}}{p C_{\mathrm{CFL}} N_{comp}} \left(\frac{L}{l_{pe}^{sw}}\right)^4 \left(\frac{L}{r_s}\right)^p L^{-3-\frac{12}{p}} \mu_o^{\frac{1}{2}+\frac{2}{p}} M^{1+\frac{4}{p}} P_d^{-\frac{1}{2}-\frac{2}{p}} \qquad (77)$$

by writing r_{mp}^{p+4} in terms of P_d and M. For numerical values of $p = 1$, $N_{sw} = 10^4$, $N_{comp} = 10^6$, $l_{pe}^{sw} = 2$ km (assumes solar wind electron density of $6.5{\cdot}10^6$ m^{-3}), L=0.1 m, $r_s = 10$ m, $M = 150$ A m^2, $P_d = 2$nPa, the computing time $T_{comp} \approx$ 65 days.

4.5 Full particle simulation

4.5.1 Number of cells and memory requirements

In a full particle simulation, the grid size is defined by the electron Debye length as

$$\Delta X = \frac{V_{th}^e}{\omega_{pe}}, \qquad (78)$$

where V_{th}^e is the thermal speed of the electrons defined as

$$V_{th}^e = \sqrt{\frac{2k_B T_e}{m_e}}. \qquad (79)$$

Similarly to the integrations in the cases of MHD and hybrid simulations, the number of cells in a full-particle simulation can be written as

$$N_c = 4\pi \left(\frac{r_{mp}}{\Delta X^{sw}}\right)^3 \ln\left(\frac{r_{mp}}{r_s}\right), \qquad (80)$$

where ΔX^{sw} is the grid size at the magnetopause given as

$$\Delta X^{sw} = \frac{V_{th}^e}{\omega_{pe}^{sw}}. \qquad (81)$$

The plasma frequency ω_{pe}^{sw} at the magnetopause is defined as

$$\omega_{pe}^{sw} = \sqrt{\frac{n_{sw} e^2}{\epsilon_0 m_e}}. \qquad (82)$$

For numerical values of $r_s = 10$ m, $\Delta X_{sw} = 15$ m (assumes solar wind electron density of $6.5{\cdot}10^6$ m^{-3} and electron temperature of 4 eV), $r_{\mathrm{mp}} = 30$ km, the number of cells $N_c \approx 6 \cdot 10^{11}$. Typically, a full-particle simulation uses about 4000 bytes per cell, which gives an estimate of $2{\cdot}10^6$ GB of memory required.

4.5.2 Time step and computing time

The time step is defined by the electron plasma frequency as

$$\Delta t = \frac{1}{\omega_{pe}}. \tag{83}$$

The number propagated cells in time T is given then as

$$N = \frac{4\pi N_{sw}\omega_{pe}^{sw} r_s}{V_{sw}} \left(\frac{r_s}{\Delta X_{sw}}\right)^3 \left(\frac{r_{\rm mp}}{r_s}\right)^5, \tag{84}$$

where ΔX_{sw} is the electron inertial length at the magnetopause. The computer time can be given as

$$T_{comp} = \frac{(4\pi)^{1-\frac{5}{p}}\omega_{pe}^{sw} N_{sw} L}{V_{sw} N_{comp}} \left(\frac{L}{\Delta X_{sw}}\right)^3 \left(\frac{L}{r_s}\right) L^{\frac{-15}{p}} \mu_o^{\frac{5}{2p}} M^{\frac{5}{p}} P_d^{-\frac{5}{2p}} \tag{85}$$

For numerical values of $p = 1$, $N_{sw} = 10^4$, $N_{comp} = 10^6$, $\Delta X_{sw} = 15$ m (assumes solar wind electron density of $6.5{\cdot}10^6$ m^{-3} and electron temperature of 4 eV), L=0.1 m, $r_s = 10$ m, $M = 150$ A m^2, $P_d = 2$nPa, the computing time $T_{comp} \approx 3{\cdot}10^{10}$ days.

4.6 Applying present-day simulation codes to magnetospheric propulsion

In general, it can be pointed out that computer simulation codes are typically highly optimized for a certain physical problem with characteristic time and length scales. Thus there are no simulation codes that would allow one to freely change the physical parameters in the simulation and study the magnetospheric propulsion effects straightforwardly.

At the Finnish Meteorological Institute, there is a global MHD simulation code for studies in the Earth's magnetosphere and a hybrid simulation code applied to magnetospheres of the inner planets. The MHD code is the only global 3D solar wind-magnetosphere-ionosphere code in Europe. Based on our experience on these simulations, we point out several facts that have to be kept in mind, when a simulation for magnetospheric propulsion effects is considered.

The parameter ranges of the Earth's magnetosphere are greatly different from those of the M2P2 magnetosphere. For example, the MHD code at FMI is highly optimized for the parameter ranges of the Earth's magnetosphere, and any adaptation of this simulation to the M2P2 system would require a substantial optimization effort, especially if the role of the magnetopause closure currents are

addressed. It can be estimated that such an adaptation would require at least 3 months of work without any unexpected complications. Even if such a simulation that would in principle be able to handle the current closure near the spacecraft will be developed, it is not evident that the simulation would result in the current pattern required for the transfer of the magnetopause force to the spacecraft.

There are several issues that have to be taken into account when adapting the terrestrial MHD simulation of FMI to the M2P2 magnetosphere:

- Boundary conditions at the inner boundary of the simulation domain.
- Mapping of the quantities between the inner boundary and the spacecraft.
- Uniqueness of the mapping under the plasma conditions near the M2P2 spacecraft.
- Impossiblity to straightforwardly initialize the M2P2 system from a vacuum field because of the large Alfvén velocity, i.e., an initial plasma density profile has to be introduced in the simulation.
- Finding an equilibrium for given solar wind parameters and the plasma profile in the simulation.
- Introduction of new plasma in the simulation corresponding to the rate of the plasma escape from the simulation.
- Current closure near the spacecraft and its dependence on the boundary conditions and mapping used.

The hybrid simulation at FMI was originally developed for the planet Mars. Later the simulation was adapted to the Hermean magnetosphere. In this case, the adaptation took a year of work. The main problem was related to the fact that the Hermean magnetic field is larger than that of the Martian magnetic field. Thus it is expected that any attempt of adapting a pre-existing planetary hybrid simulation will run into problems with the large magnetic field magnitudes of the magnetospheric propulsion concepts. It has also to be kept in mind that the equations for a hybrid simulation cannot be written in a conservative form. This results in numerical instabilities in the simulation, which typically leads to unlimited growth of energy, especially the magnetic energy.

Based on the above estimates on the required computing times, full-scale particle simulations must be considered as future refinements of the results deduced by MHD or hybrid simulations.

5 Technology requirements for magnetospheric propulsion

The topic of this section is to consider whether technology is available to build a magnetic propulsion system that can provide a space exploration mission with the speed of at least 10 AU yr^{-1}. For this purpose we look at the technology requirements for space-based and ground-based demonstrations of magnetospheric propulsion and qualitatively evaluate to what extend the prototype would model a full-scale mission.

5.1 The most critical parameters

As discussed above the primary technological issue for PFMP is related to the large magnetic moment of the current coil attached to the spacecraft. Thus two critical parameters are:

- Spatial dimension of the superconducting coil.
- Current density of the superconducting coil.

According to Section 3, current density of the order of 10^{10} Am^{-2} is required for a current loop with a radius of 100 km in order to create a magnetic moment large enough to produce an acceleration of 0.01 m s^{-2} for a full-scale mission. An increase of the maximum current density to 10^{11} A m^2 allows a reduction of the current coil radius from 100 km to 1 km. This underlines the key role of the maximum current density allowed by the superconducting material.

According to the scaling laws derived in Section 2 only a fraction of the force acting on the magnetopause is transferred to the spacecraft by the magnetopause currents. However, as discussed in Section 2 it might be possible to transfer part of the force to the spacecraft by currents partially closing the magnetopause currents near the spacecraft. However, this has to take place very close to the spacecraft and this implies two critical issues for the M2P2 concept:

- Current closure distance from the spacecraft.
- Plasma pressure and density at the closure region.

In the case a M2P2 full-scale mission, the generation of the magnetic field is not critical, and a size of a magnetopause comparable to the size of the PFMP

magnetopause can in principle be created using an ohmic coil. Based on the results of Section 3, in order to transfer the magnetopause current fully to the spacecraft the magnetopause current has to close at a distance of 20 cm from the spacecraft. This would require a plasma number density of 10^{20} m^{-3} at the spacecraft. The efficiency of the closure currents in transferring the force on the magnetopause due to the solar wind pressure decreases very fast as a function of the distance from the spacecraft. By increasing the magnetic moment attached to the spacecraft and assuming a magnetic field decay power of 2, the currents could be closed at more realistic distances with lower plasma density than implied by the decay power of 1. However, the higher the magnetic field is near the spacecraft the more difficult it is to produce high-density near the spacecraft. The the key element in developing the M2P2 concept is the plasma source.

5.2 Evaluation of the technology

5.2.1 PFMP full-scale mission

Cooling of the superconducting coil depends on the type of the superconducting material. According to the critical temperature, the superconductors can be divided into two categories, Low-Temperature Superconductors (LTS) and High-Temperature Superconductors (HTS). Feasibility of such materials for magnetic propulsion depends on the cooling systems available for reaching the superconducting state. The cooling can either be passive or active.

Passive cooling in space can be realized by coating the superconducting wire with semi-transparent material that reflects the solar radiation, but passes the black body radiation from the superconductor. Such materials exist and they can be categorized by their α-to-ξ ratio defined by the rates of absorbed and radiated heat. The equilibrium temperature can be expressed as

$$T = \left(\frac{A_s}{A} \frac{\alpha}{\xi} \frac{J_s}{\sigma} \right)^{1/4} , \tag{86}$$

where A is the black-body radiating surface, A_s is the surface absorbing the solar radiation, J_s is the solar constant (1350 W m^{-2}), and σ is the Stefan-Boltzmann constant ($5.67{\cdot}10^{-8}$ W K^{-4} m^{-2}). If one assumes a cylindrical wire $A_s/A = 0.5$. For the best materials, the α-to-ξ ratio is about 0.08, which gives temperature of 175 K at 1 AU. The highest known critical temperatures for superconductive state are up to 160 K. However, such temperatures cannot yet be reached in practice, and passive cooling can be expected to work at most around Jupiter or Saturn. Since the dynamic pressure of the solar wind decreases in distance r as r^{-2}, the superconducting state has to be reached closer to the Sun, at least at 1 AU in order a mission based on the PFMP concept to work.

The actually manufactured superconducting wires have a tape-like shape, which may reduce the A_s-to-A ratio down to 0.05, if a superconducting tape with thickness of 0.2 mm and width of 4 mm is configured in such a way that the tape surface is perpendicular to the spacecraft-Sun line. Such a configuration would reduce the equilibrium temperature down to 100 K. In the near future, it is possible that new materials will be developed, but presently active cooling has to be applied to maintain the superconductivity at radial distances closer than 1 AU.

Using cryogenic Helium cooling, the operating temperatures of LTS materials can be reached. The materials with the critical temperature above 77 K, i.e., HTS materials can be cooled by cheap and readily available liquid Nitrogen. A convenient and technically feasible way to accomplish active cooling is to use a hollow wire with liquid Nitrogen flowing inside the wire. However, using any active cooling system will increase the total mass of the spacecraft and reduce the efficiency of the PFMP concept.

Figure 19 shows the progress in the superconducting materials. Even though the critical temperatures for Mercury-based materials are up 160 K, the critical temperatures for materials used in manufacturing superconducting wires are lower. There are two HTS wire architectures: Multi-filamentary composite (MFC) and coated conductor composite (CCC). Presently, one of the highest performing HTS wire capable of carrying over 140 times the power of copper wires of the same dimensions is manufactured by American Superconductor, AMSC (http://www.amsuper.com/html/). The current density is about $1.6{\cdot}10^8$ A m^{-2}, and the coil radius should be several tens of kilometers in order to gain a magnetic moment large enough for PFMP. However, these wires are produced in pieces up to 200 m.

Very high levels of current carrying performance have been reported in laboratory samples of second generation HTS coated conductor composite wires. Recently, AMSC reported that that a 10-meter-long CCC wire made of Yttrium compound was successfully tested. The liquid-metal-organic deposition (MOD) technique was used for producing the HTS coating, which is inherently a high-volume, low-cost manufacturing technique.

The maximum current density remains as one of the key characteristics of the superconducting wires to be improved in addition to the operating temperature and tolerance to the surface magnetic field magnitude. For LTS materials, the critical current density and magnetic field are presently higher than those of HTS materials. Furthermore, longer wires can be produced using LTS materials. However, LTS materials are beyond the temperature range achieved by passive cooling in the interplanetary space, and thus presently the PFMP concept is not technically feasible. However, the rapid progress in development of superconducting wires implies that superconducting wires with critical parameters sufficient for

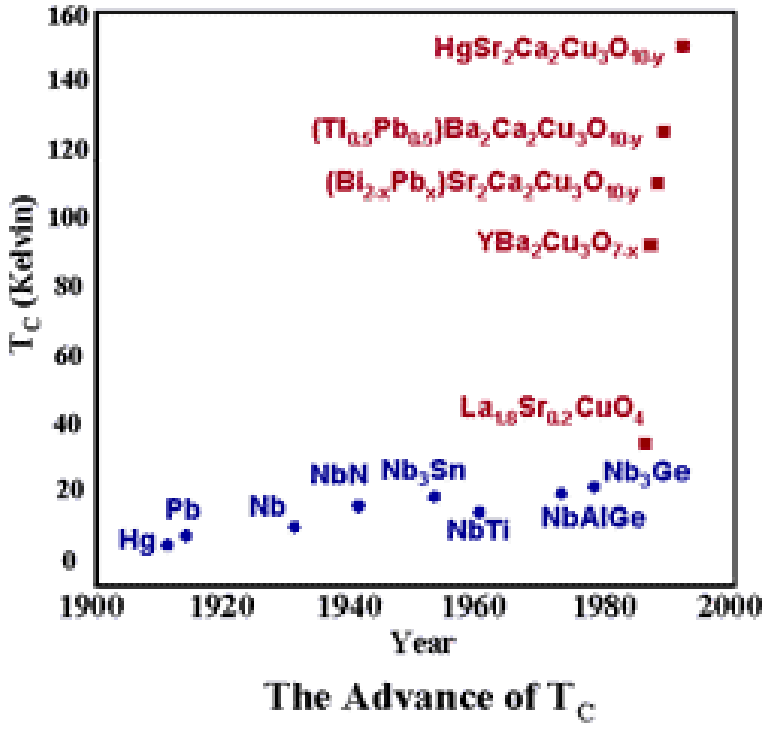

Figure 19: The advance of the critical temperature of the superconducting materials

the PFMP concept may well be available in the near future.

5.2.2 M2P2

Considering a full-scale mission based on the M2P2 concept, the most critical technical issue is the plasma source, whereas an adequate magnetic field can be achieved even using traditional ohmic coils. The plasma source of M2P2 has to produce plasma at high β, at high efficiency, and at multikilowatt power level. Such a source exists and is based on a Rotating Magnetic Field (RMF) [*Slough and Miller,* 2000]. The induced plasma currents driven by RMF ionizes and heats the plasma. The RMF source is an inductively coupled source like the Helicon, but has no power, plasma density, or temperature limitations.

In a space-based demonstration of M2P2, the key issue is to measure the acceleration of the demonstrative spacecraft. Here, we consider three options relevant for such a measurement: accelerometers; pulsed laser rangefinder; and laser in-

terferometry. In addition, it is desirable that also any rotation of the spacecraft due to possible torque induced by the solar wind could be obtained.

There are already available accelerometers that fulfill the requirements for space-based demonstration. For example, ultra-sensitive space accelerometers manufactured by ONERA in France has sensitivity of the order of 10^{-9} m s^{-2} (http://www.onera.fr/dmph-en/accelerometre/index.html). Furthermore, ultra-sensitive accelerometers are further developed, for example for the purposes of the Laser Interferometry Space Antenna (LISA) mission. In the LISA mission, accelerometers with a noise level of 10^{-14} m s^{-2} are required.

Pulsed Laser Rangefinders (PLR) are based on the time-of-flight measurement of laser light between the spacecraft and target, which sets up strict requirements for the instrument electronics. Recently, a PLR device was used in the Near Earth Asteroid Rendezvous (NEAR) mission to measure the distance between the NEAR spacecraft and the asteroid Eros. The range of the Near Laser Rangefinder (NLR) was up to 50 km with an accuracy of 6 m. Such an accuracy range corresponds to a time period of 3 hrs for an acceleration level of 10^{-7} m s^{-1}. These numbers imply that in space-based demonstration of the magnetospheric propulsion concepts only the long-term averaged propulsive effect can be studied: the effects of the solar wind variability to the spacecraft propulsion cannot be resolved (a spatial accuracy of about 1 cm corresponds to a time scale of about 7 min). Thus based on already existing technology on space-borne rangefinders the acceleration feasible for a space-based demonstration cannot be measured up to the desired accuracy.

Laser interferometry has been considered to be applied in the positioning system of the LISA mission. In this mission, three spacecraft form a large-scale Michelson interferometer with a spatial scale of about $5 \cdot 10^6$ km. The LISA mission aims at a spatial accuracy of 10^{-11} m that would be by all means sufficient for the space-based demonstration of magnetospheric propulsion concepts.

5.2.3 Magnetic shielding

As the magnetospheric propulsion concepts corporate large magnetic fields, the electric devices may have to be magnetically shielded. The shielding can be arranged by 1) spatial shielding, i.e., locating the current coil as a ring around the spacecraft at an adequate distance to provide the electronics with a magnetically suitable conditions; 2) magnetic shielding based on high-permeability materials; or 3) magnetic shielding based on permanent magnets.

The first method is characteristic for the PFMP concept, if a full-scale mission is considered as only magnetic field magnitudes of the order of 10^{-6} T are expected

at the spacecraft (Table 1). However, such a spatial shielding is not necessarily enough for a M2P2 full-scale mission (0.06 T; Table 1) and space-based demonstrations in the solar wind (Table 3, see Section 6). An important fact that has to be kept in mind when considering a spatial shielding in the case of M2P2 is that the current coils are subject to a large heat flux from the injected plasma.

The shielding material has to have a relatively large saturation induction rating in order to shield from a large magnetic field. Such materials cannot achieve high magnetic permeability levels of low saturation materials, and the magnetic attenuation of these materials is only moderate. However, an attenuation of the magnetic field by a factor of 10 would already permit operation in magnetic fields of a few mT in the cases when the spatial shielding is not adequate (Table 3).

In the case of the PFMP demonstration with a superconducting coil in the solar wind, the shielding with high-permeability materials may not be enough (Table 3). In this case, magnetic shielding can be realized by using permanent magnets with a large magnetic field with spatial scale sizes small relative to those of the gradients of the magnetic field of the main current coil.

5.2.4 Laboratory demonstration

Several laboratory experiments on magnetospheric physics have been carried out in the past, for example by *Minami et al.* [1993] and *Rahman et al.* [1989].

Minami et al. [1993] studied the earthward electric field in the equatorial current sheet in a laboratory simulation experiment of the Earth's magnetosphere. The experiment was carried out at the Osaka City University. An artificial solar wind with a velocity of $7{\cdot}10^4$ m s^{-1} and Argon plasma with plasma density of 10^{19} m^{-3} was injected in a vacuum chamber for about 100 μs by a coaxial plasma gun. The spatial scale of the plasma chamber were 0.6 m in diameter and 1.7 m in length. These numbers imply that the simulated solar wind passed the chamber length about 4000 times in 100 μs. The strength of the dipole magnetic field simulating the internal geomagnetic field was 0.8 T.

Rahman et al. [1989] made a laboratory experiment to study the formation of the large-scale Birkeland current system in the polar region of a demonstrative globe. The solar wind was simulated by a coaxial plasma gun which generated a Hydrogen plasma pulse of approximately 100 μs duration flowing through a plasma drift chamber with spatial dimensions of 1.3 m in diameter and 11 m in length. Table 2 summarizes the parameters used in the experiments.

Based on the parameters used in the laboratory experiments described above, the ground based demonstration of the magnetospheric propulsion concepts is

Parameter	Space	Laboratory
Solar wind parameters		
Solar wind flow velocity [m/s]	$4{\cdot}10^5$	$1.5{\cdot}10^5$
Plasma density [cm^{-3}]	5	$5{\cdot}10^{13}$
Interplanetary magnetic field [T]	$5{\cdot}10^{-9}$	$2.5{\cdot}10^{-2}$
Alfvén Mach number [1]	8	2.75
Spacecraft parameters		
Radius [cm]	10	2.75
Magnetic field at the equator [T]	0.06	1.8
Magnetic moment [A m^{-2}]	315	400

Table 2: Laboratory parameters used by *Rahman et al.* [1989] in comparison with the solar wind and full scale parameters of M2P2.

feasible in pre-existing plasma laboratories.

In the experiment of *Minami et al.* [1993], an artificial magnetosphere with a realistic shape of the magnetopause 7 cm upstream from the demonstrative globe was created (their Figure 1). The plasma density and velocity of the simulating solar wind corresponds to a dynamical pressure of about 2000 Pa. Such a dynamical pressure inserts a force of about 30 N on a magnetopause with a scale length of 7 cm. If the artificial magnetosphere of the magnetospheric propulsion concepts can be created and maintained under such dynamic pressure conditions, the force acting on the demonstrative spacecraft can be measured.

6 Prototyping

6.1 Prototype mission in the solar wind

Based on the parameter ranges presented in Section 3, it is possible to demonstrate both PFMP and M2P2 concepts in a single mission. It is also important for understanding the concept of magnetospheric propulsion to have a possibility to turn of the plasma source and the magnetic field to reset the system for testing the PFMP concept with a vacuum magnetic field. In Table 3 we have collected a suggestion for baseline parameters for a solar wind demonstration of both PFMP and M2P2 concepts utilizing both ohmic and superconductive coils.

Key parameters	**PFMP**	**M2P2**	**PFMP**	**M2P2**
Coil	Ω	Ω	SC	SC
Diameter [m]	20.0	20.0	2.0	2.0
Thickness [mm]	2.0	2.0	3.0	3.0
Current [A]	9.4	$3.2{\cdot}10^{-2}$	299.0	9.5
Mass [kg]	1.8	1.8	1.8	1.8
Magnetic moment [A m^2]	$9.4{\cdot}10^2$	10.0	$9.4{\cdot}10^2$	30
Magnetic field [mT]	5.9	0.02	1900	59.7
Ohmic power [W]	29.5	$3.4{\cdot}10^{-4}$	-	-
Cooling power [W]	-	-	3.1	?
Plasma				
Density [m^{-3}]	-	10^{17}	-	10^{17}
Power [W]	-	36	-	36
Acceleration [m s^{-2}]	10^{-6}	10^{-4}	10^{-6}	10^{-4}

Table 3: A suggestive baseline set of parameters for a demonstration in the solar wind for PFMP and M2P2 using either an ohmic (Ω) or superconducting coil (SC). The power associated with the plasma production of M2P2 is the peak power consumed in production 4-keV argon plasma [e.g., *Winglee et al.*, 2000]. The long-term power consumption depends on the rate at which the plasma escapes from the system and cannot be estimated at the level required for a number estimate. The accelerations given assumes a total mass of the demonstrative satellite of 360 kg. Due to active cooling, the superconducting coil is a pipe with a shell thickness of 0.38 mm. The cooling power given here corresponds to a black body radiation power difference between 175 K and 70 K. In the case of M2P2, the injected plasma complicates the cooling and no explicit power estimate is given here.

6.1.1 Configuration

Based on the available technology on space accelerometers, pulsed laser rangefinders, and laser interferometry, the prototype mission can consist of either one or two spacecraft: In a single satellite mission, the acceleration can be measured by an accelerometer, but the solar wind condition and the configuration of the artificial magnetosphere cannot be probed. Thus it is favorable to use two satellites in such a way that one of the spacecraft (spacecraft A) has the magnetic field coil attached to it and the second spacecraft (spacecraft B) can monitor the solar wind conditions and also fly through the artificial magnetosphere to probe the plasma conditions and the magnetopause location and structure. Such a set up provides us with a possibility of full parametric study of the magnetospheric propulsion. The use of two satellites also allows the use of a pulsed laser rangefinder or laser interferometry. In the case of a single spacecraft mission, the accelerometer has

to work in a strong magnetic field which may complicate the construction and operation of the accelerometer.

6.1.2 Instruments

Minimum set of instruments on board the spacecraft A, i.e., equipments that are required for the study of the propulsion includes:

- Magnetic coil
- Plasma source
- Accelerometer

For the spacecraft B, the minimum set can be listed as

- Rangefinder
- Particle detector
- Accelerometer
- Magnetometer

The accelerometer on the spacecraft B allows an absolute determination of the acceleration of the spacecraft A, and the magnetometer allows studies of the effects of the solar wind magnetic field on the size and configuration of the artificial magnetosphere around the spacecraft A. In addition the magnetometer gives important information of the magnetic field and currents in the artificial magnetosphere during fly-throughs.

Table 4 shows the masses and power consumption of the baseline instrumentation given above. The mass and power estimates are based on pre-existing spacecraft instruments. The cost estimates given are statistical and based on the mass of the instrument. For more information, see the caption of Table 4. Since there are some unknown details related to the actual instruments implemented in each particular cases, these estimates may contain substantial uncertainties. Especially, there are no ways of estimating the real cost of the plasma source with the unknown issues arising from the simultaneous operation of strong magentic fields and dense plasma.

Instrument	Power[W]	Mass[kg]	Cost[MEURO]
Spacecraft A			
Magnetic ohmic (SC) coil	30 (3)	2 (2)	3 (3)
Plasma source	36	20	10
Accelerometer	16	9	7
Total	82 (55)	31	20
Spacecraft B			
Rangefinder[1]	5	21	5
Particle det.[2]	14	16	9
Magnetometer[3]	4	1	4
Accelerometer	16	9	6
Total	39	47	24

Table 4: Baseline instrumentation of the spacecraft A and B with suggested mass and power. The mass and power information of the spacecraft B:
http://www.msss.com/small_bodies/near_new/nlr.html[1],
ftp://sierra.spasci.com/DATA/timas/TIMAS_description.html[2], and
http://www-ssc.igpp.ucla.edu/polar/mfedescrip.html[3].
The cost estimation are statistical based on the mass of the instrument as given at http://www.jsc.nasa.gov/bu2/SVLCM.html. The prices are converted to euros with an exchange rate of 1.0 (note the numbers are from the year 1999) and rounded. The mass of the plasma source at the spacecraft A is a guess without realistic basis.

6.1.3 Additional equipments

There are several additional equipments to be included in the spacecraft A and B. In the case of the magnetic coil being a superconducting wire, an active cooling system has to be added to the spacecraft A. Furthermore, a power supply for the coil, plasma source, and accelerometer are needed. If the large magnetic field or, especially, the injected plasma undermines the use of solar panels, the power supply has to be a battery or the power can be transferred from the spacecraft B. As the current source for the magnetic coil was proposed to be variable, the solar panels could be used to charge the battery when the magnetic field is turned off. Thus the spacecraft A has to be equipped either with a battery and solar panels or a receiver for the power transfer from the spacecraft B. Finally, the spacecraft A has to have a receiver and transmitter for data and operational commands. Additional equipments for the spacecraft B include solar panels and receivers and transmitters for communication with the spacecraft B and ground station. If the power for the spacecraft be is considered to be transmitted from the spacecraft B, for example as a laser beam, such an transmitter is to be added in the spacecraft B. Note that such a scheme could probably be applied in

determining the distance of the spacecraft A from the spacecraft B and thus the acceleration of the spacecraft A.

6.1.4 Cost estimates

As some key elements of the technology associated with the space-based demonstration mission are not fully fixed, realistic costing details for such a mission are difficult to obtain. Based on the instrument cost estimations presented in Table 4, it can be expected that the demonstration can be realized using one or two SMART-class spacecraft, about 100 Meuro per satellite, with an instrumentation of the order of 20-30 Meuro per each spacecraft. In addition, there will be the normal launch and operation costs.

6.1.5 Qualitative assessment of the prototype

The artificial magnetosphere has smaller spatial scales and lower level of acceleration than that of the full-scale mission. It can be argued that it models the essential physics of a full-scale mission: the same plasma approximations valid for the full-scale mission are also valid for the prototype.

An important issue of the prototype is that the effects of the solar wind variations to the propulsive effect can be measured. At this point, estimates on the response time of the M2P2 artificial magnetosphere to the solar wind variations cannot be made, and the feasibility of the present instruments obtaining the spacecraft acceleration is not a trivial issue. For example, possible effects of the solar wind variations on the spacecraft attitude may complicate the range measurements based on laser techniques.

6.2 Prototype in a vacuum chamber

The parameter ranges achieved in the present-day plasma laboratories set no critical limits to ground-based demonstration of the magnetospheric propulsion concepts. In fact, the concept of PFMP can be simulated using an experimental setup similar to that of *Minami et al.* [1993]. In the case of M2P2, the magnetic moment has to be scaled down to be of the order of 20 A m^2 to create an artificial magnetosphere with a size similar to those ($\sim$ 10 cm) of the experiments carried out by *Minami et al.* [1993] and *Rahman et al.* [1989]. The exact value of the magnetic moment depends on the plasma used to simulate the solar wind flow and, especially, the magnetic field decay power p. Since the size of the

artificial magnetosphere depends strongly on p, the magnetic moment used in the simulation has to be variable in a range from 20 ($p = 1$) to 80 ($p = 2$) A m^2. Furthermore, the time scale of these simulations (100 μs), which is adequate for formation of the artificial magnetosphere, sets the upper limit for the time scale required for the stability of the M2P2 inflated magnetosphere.

It should also be pointed out that there are two principle procedures for the inflating of the artificial magnetosphere and inclusion of the artificial solar wind: 1) the magnetosphere is first inflated in vacuum and then the wind added; or 2) the inflation takes place under the artificial solar wind dynamical pressure. Both procedures are complicated. In the former case, the size of the artificial magnetosphere has to be extensively large in the vacuum to maintain an adequate size when the wind is switched on. This is not possible due to the limited diameter of the vacuum chamber. In the latter case, the wind pressure pushes the magnetopause very close to the demonstrative spacecraft, and the injection of the plasma to the closed field lines in the vicinity of the spacecraft and the inflation of the magnetic field may be troublesome due to the large magnetic field magnitudes near the spacecraft. Thus, it is most probable that an intermediate method between these two procedures must be used: the wind pressure is gradually enhanced as the dipole field is being inflated.

6.2.1 Qualitative assessment of the prototype

Based on the simulation results by *Minami et al.* [1993] and *Rahman et al.* [1989] it can be expected that a ground-based prototyping of the propulsive effects gives valid information of the physics of the magnetospheric propulsion systems. In both cases, an artificial magnetosphere that resembles the shape of the Earth's magnetosphere was created. Furthermore, both of these simulations showed that the plasma and field parameters can be measured inside the artificial magnetosphere: *Minami et al.* [1993] were able to study the formation of the tail plasma sheet and the earthward electric field in the simulated plasma sheet; and *Rahman et al.* [1989] were able to access the large-scale Birkeland current system in the polar region of the globe used in their simulation. In the case of M2P2, the transfer of the solar wind pressure force acting on the magnetopause to the spacecraft is critical. As this transfer most likely takes place via field-aligned currents that close in the vicinity of the spacecraft, the results of *Rahman et al.* [1989] are of essential importance for the validity of the laboratory testing of the M2P2 concept.

7 Discussion and conclusions

In this report we have discussed several aspects of magnetospheric propulsion. The basic idea of the magnetospheric propulsion is to create an artificial magnetosphere around a spacecraft by using large magnetic fields. The magnetosphere is separated from the solar wind by a magnetopause that deviates the solar wind around the magnetosphere. In other words, the magnetosphere absorbs momentum of the solar wind, and some fraction of this momentum can push the spacecraft. There are two ways of establishing the propulsion: one is to deploy a vacuum magnetic field by current coils attached to the spacecraft (PFMP) [*Zubrin,* 1993]; and the other is to further inflate the magnetic field by injecting plasma into the magnetic field (M2P2) [*Winglee et al.,* 2000].

The ultimate purpose of the study was to assess the feasibility of the magnetospheric propulsion. This requires the identification of the the force transferred from the solar wind to the spacecraft, estimation of its strength, and evaluation of technological requirements to be fulfilled.

In this study we have not at all dealt with problems associated to navigation. Solar wind is much more variable than the steady flux of solar photons. It is evident that solar wind sailing to a given destination would be much more difficult than more traditional solar sailing.

7.1 Theoretical results

The force acting on the spacecraft, or more exactly, on the current coil attached to the spacecraft is the Lorentz force caused by the external magnetic field arising from the current systems of the artificial magnetosphere. The current systems are induced by the interaction of the magnetosphere with the solar wind. One of the main results of this study is a set of scaling laws for the key parameters of the investigated propulsion systems.

In the case of PFMP it is straightforward to show that the force acting on the spacecraft is the same as the force acting on the magnetopause by the dynamic pressure of the solar wind. The reason for this is that there are no other sinks of the solar wind momentum in the system, as the magnetosphere is empty.

In the case of M2P2 we have shown that the force on the magnetopause and the force on the spacecraft due to the magnetopause current are vastly different. A physical explanation for this is that there is a third massive body in the system, in addition to the solar wind and the spacecraft, the injected plasma. The injected plasma carries away a large fraction of the solar wind momentum as it escapes

from the system to the solar wind. This is an important result concerning the further development of M2P2, because it implies that residual force acting on the spacecraft may be orders of magnitude weaker than the force exerted by the solar wind on the magnetopause. In fact, we have demonstrated that if the magnetopause current were the only current system to create the Lorentz force, only a fraction of 10^{-10} of the force on the magnetopause would be transferred to the spacecraft. Currents inside magnetosphere may increase this fraction but in order to create significant forces, strong currents must flow within centimeters of the spacecraft, which, in turn, requires large plasma densities close to the spacecraft.

The hypotheses to come to these conclusions were the following:

- The MHD approximation is valid up to an accuracy of one order of magnitude.
- The magnetopause currents form the primary current system.
- The primary length scale of the force generated by the magnetopause currents is the subsolar distance R_{MP}.
- The magnetopause currents are partially closed near the spacecraft.
- The currents possibly closing near the spacecraft introduce an additional scale lenght to the M2P2 system and contribute to the transfer of the force on the magnetopause to the spacecraft.
- The force on the spacecraft generated by the closure currents can be estimated from the Biot - Savart law.

Our theoretical study is by no means complete and the following issues can be listed as unsolved after the present project:

- Validity of the MHD approximation.
- Formation of the magnetopause beyond the MHD scale.
- Large-scale stability of the injected plasma of M2P2.
- Amount and momentum of plasma escaping from M2P2.
- Is a closure of the magnetopause currents possible near the M2P2 spacecraft.
- Issues related to orientation of the dipole axis (*e.g.*, spinning of the spacecraft)

7.2 Parametric results

We have studied parameter ranges for full-scale mission, space-based demonstration, and ground-based demonstration of both PFMP and M2P2 concepts. In the case of a full-scale mission an acceleration of 0.01 m s^{-2} is required for the spacecraft to gain the desired speed of 50 km s^{-1}. For a space-based demonstration, we considered an acceleration of 10^{-9} m s^{-2} as the minimum acceleration. Such a lower level of acceleration allows the spatial scales of the current coil attached to the PFMP spacecraft to be smaller by a factor of about $3{\cdot}10^3$ (for a given current density) than the coil size of a full-scale mission. The main issue of the M2P2 concept is whether such a current system, that transfers the force acting on the magnetopause to the spacecraft, can be generated in the interaction between the M2P2 magnetosphere and the solar wind. We considered an M2P2 magnetosphere having a magnetopause cross-section of the same size as the PFMP magnetosphere. We assumed that the magnetopause current is partially closed near the spacecraft, and the magnetopause force is then transferred by such a current system. The distance of the closure region from the spacecraft is the main parameter to study for the demonstration of M2P2.

We investigated demonstrations of the propulsive effects of PFMP and M2P2 both in the ionosphere and in the solar wind. In the ionosphere, the drag caused by the dynamical pressure of the neutrals to the spacecraft body is of the same order than the drag generated by the charged particles against the magnetopause of the demonstrative spacecraft. In addition, the magnetic force induced by the Earth's magnetic field has to be removed from the drag measurements. Since the magnetic field pressure of the Earth's magnetic field (0.6 mPa) is larger than the dynamic pressure (10 nPa), the size of the magnetosphere of the demonstrative spacecraft is defined by the Earth's magnetic field alone. Based on these arguments, we anticipate that the ionospheric demonstration is not realistic for demonstrating the propulsive effects of the magnetospheric propulsion concepts. However, the ionospheric demonstration may be interesting for studies of spacecraft re-entry to the atmosphere, but the propulsive effects have to be demonstrated in the solar wind.

For completeness, we considered three options for generating the magnetic field around the spacecraft:

- Superconducting wire.
- Ohmic wire.
- Permanent magnet.

The major pros and cons of the options above can be listed as:

- Use of superconducting wire requires an active cooling system for the current coil attached to the spacecraft orbiting the Earth.
- Use of superconductors allow larger current densities than those feasible for ohmic conductors.
- Both superconducting and ohmic wires allows variation of the current density and thus the acceleration of the spacecraft.
- The ohmic (Joule heating) and superconducting (cooling system) coils requires external power from the spacecraft.
- Use of permanent magnet does not require any power to maintain the magnetic field.
- Use of permanent magnets assumes large magnetic field values at the surface of the permanent magnet and may lead to complications at the launch of the spacecraft.
- Permanent magnet is passive, and cannot be used for studies of different magnetic field strengths.

Based on the above considerations, we conclude that the permanent magnets are not suitable for the space-based demonstration, and only the current coils were considered further.

On the ground, the propulsive effects of the magnetospheric propulsion concepts have to studied in a vacuum tank. The large magnetic field used in confining the plasma in a plasma chamber generates large forces on the current coil that creates the magnetopause around the spacecraft. An artificial solar wind can be produced, for example by a coaxial plasma gun. Here, we studied the density of the plasma generated by the plasma gun versus the speed of the artificial solar wind in order to gain a net force that can be measured in the vacuum tank.

We conclude that the parameter ranges deduced here for the space-based and ground demonstrations are very promising, and that the propulsive effects of both PFMP and M2P2 can be studied using such demonstrations.

7.3 Computer simulations

We have estimated computer memory and computing time requirements for MHD, hybrid, and full-particle simulations. In all estimates the state-of-the-art

adaptive grids are assumed. These estimates assume a certain radial dependence of the magnetic field and the plasma density of the M2P2 magnetospheric plasma. The computing time depends strongly on the radial distance of the inner boundary of the simulation domain from the spacecraft. This is due to the fact that the time step decreases strongly as a function of the increasing magnetic field close to the spacecraft.

Based on the estimates derived here for an MHD simulation, the M2P2 system can, in principle, be simulated. However, the inner boundary of the simulation domain may not be as close to the spacecraft as required for an adequate transfer of the magnetopause force to the spacecraft as deduced from the parametric estimates. Note further, that optimization of any pre-existing magnetospheric MHD code to the case of M2P2 is not a trivial task. We anticipate that the programming would require three months of work without any unexpected numerical complications caused by the large ranges of scale lengths of M2P2. Furthermore, the validation, documentation, and actual simulations adds up to this estimate, and it can be expected that at least a total amount of work of one year would need to be allocated for such a simulation project. One should also understand that it is not evident that the simulation would generate a current system that closes near the spacecraft, even if that would be the case in reality. Furthermore, the simulation would still be based on MHD.

The estimates for the requirements for a hybrid simulation are also encouraging. However, based on our experience on hybrid simulations in planetary magnetospheres, the large magnetic field magnitude associated with the M2P2 concept would likely lead to considerable complications in practical application of a hybrid simulation on the M2P2 magnetosphere.

Finally, it is evident that any attempt of applying full particle simulation to the M2P2 system is beyond the present computer capacities.

7.4 Evaluation of technology

The most critical technical issue of the PFMP concept is the superconducting coil with spatial scale of tens of kilometers required for the artificial magnetosphere around the spacecraft. The cooling of such a wire would in practice need to be passive. In principle, an active Helium (LTS materials) or Nitrogen (HTS materials with critical temperature above 77 K) cooling might be used, but it will reduce the efficiency of the PFMP propulsion by increasing the total mass of the spacecraft. Using passive cooling (covering the superconducting material with semi-transparent material) the wire can be cooled down to 175 K at 1 AU. Since the materials with such high critical temperatures are not yet available,

the passive cooling can be expected to work at distances of Jupiter or Saturn. However, the solar wind dynamic pressure decreases rapidly as a function of the distance from the Sun, and it is essential that the magnetospheric propulsion can be used close to or even below 1 AU. Thus presently the PFMP concept is beyond the technology on superconducting wires. However, the rapid advances in development of superconducting wires suggest that superconducting wires with critical parameters sufficient for the PFMP concept may well be available in the future.

The plasma source for the M2P2 has to be able to produce plasma with high enough number density in presence of a large magnetic field. Such a source exists and is based on the concept of Rotating Magnetic Field (RMF). The plasma is ionized and heated by induced plasma currents driven by RMF. Such a source is an inductively coupled source like the helicon and has no power, plasma density, or temperature limitations.

In order to demonstrate the magnetospheric propulsion concepts of PFMP and M2M2, no high-performing superconducting wires nor advanced plasma sources are required, but accurate enough instruments to measure the acceleration of the demonstrative spacecraft are needed. Such measurements can be obtained by accelerometers, pulsed laser range finders, or positioning system based on laser interferometry. There are already available ultra-sensitive (10^{-9} m s^{-2}) space accelerometers. In addition to an accelerometer on board the spacecraft demonstrating the propulsion, the acceleration can be measured by using another spacecraft that would be useful also for monitoring the solar wind and the plasma parameters of the artificial magnetosphere of the demonstrative spacecraft. The second spacecraft can be equipped with the above laser-based systems.

Several laboratory experiments on magnetospheric physics have been carried out in the past by elaborating plasma or vacuum chambers. Based on such experiments, we conclude that both PFMP and M2P2 can be tested on the ground. Technically, this is based on the fact that in addition to large enough plasma flow velocities, the plasma guns used in such experiments can produce sufficient plasma density to provide dynamic pressure large enough for studies on magnetospheric propulsion. In order to complete the laboratory approach to the magnetospheric propulsion, the force acting on the demonstrative apparatus situated in the chamber has to be measured. Based on the velocities and densities achievable using plasma guns and drift chambers, dynamic pressure up to 2000 Pa can be generated (force 30 N to an effective magnetopause surface of radius of 7 cm). This implies that in principle the force can be measured, if the artificial magnetosphere remains stable under such a dynamical pressure of the artificial solar wind.

7.5 Prototyping

For a prototype mission in the solar wind, it is important that the magnetic field and plasma source supporting the artificial magnetosphere can be turned off in order to study both PFMP and M2P2 during a single mission: while the study of PFMP can simply be during a single deployment of the artificial magnetosphere, the inflation of the M2P2 magnetosphere is worthwhile to execute under different solar wind conditions. In order to achieve a complete set of measurements on the physics of the M2P2 concept, we suggest that a pair of spacecraft is used. One of the spacecraft (A) has a minimum payload of a magnetic coil, plasma source, and accelerometer. The other (B) carries at minimum a pulsed laser rangefinder and particle detector. Spacecraft B is important for a full understanding of the effects of the solar wind conditions on the propulsion, as it can monitor the solar wind outside the magnetosphere of spacecraft A. In addition to the solar wind monitoring, it may execute several fly-throughs to monitor the magnetopause location and structure and the plasma parameters inside the magnetosphere. A magnetometer on board spacecraft B would allow measurements of the magnetic field and thus information of the current flowing inside the artificial magnetosphere. Finally, we argue that such a prototype with reduced scale sizes would model an actual full-scale mission. This is mainly because it works under the same class of plasma approximations of typical solar wind parameters as the full-scale mission.

There have been several laboratory experiments made on magnetospheric physics using parameter ranges applicable also for ground-based prototyping of the magnetospheric propulsion concepts. Since several of them elaborate dipole field either in a vacuum or in a drift chamber, the prototyping of the PFMP can be based on already existing laboratory set-ups. Furthermore, based on relevant results of such experiments, it can be anticipated that essential information for further applications of PFMP can be acquired this way. In the case of M2P2, any laboratory experiment is far more complicated. This is mainly because of the inflation of the artificial magnetosphere. Inflation of a vacuum dipole magnetic field with a magnetic moment required for testing the propulsive effect under the influence of the plasma flow leads to spatial scales larger than available vacuum chambers. On the other hand, inflation of a dipole under influence of the plasma flow implies that the inflating plasma has to be injected to a strong magnetic field, as the dynamical pressure of the plasma flow pushes the magnetopause very close to the dipole. Thus it was suggested that the dynamic pressure of the plasma flow has to be gradually increased from zero while the artificial magnetosphere of M2P2 is being inflated. As for PFMP, it can be expected that laboratory experiments will provide us with essential new information on the physics of the M2P2 concept. Especially, it is important to acquire any information on the transfer of the force from the magnetopause to the spacecraft via field-aligned currents closing in the vicinity of the spacecraft.

7.6 Final comments

The acronym eMPii (pronounced as em-pee) is an expression in the Finnish language that can be translated as "he/she hesitates". When we thought about a bid for this project, we already were aware of the flaws in *Winglee et al.* [2000] and hesitant about the whole concept of magnetospheric propulsion. This was also made clear in our proposal that was, nevertheless, accepted by ESA. The first actual analyses based on the force by magnetopause current described in Section 2 turned out to be even more pessimistic than we had anticipated. At the same time it became clear that the details of the system are really complicated and their full assessment is beyond simple theoretical reasoning. After all, an artificial magnetosphere is expected to be a whole new plasma world whose complexity and range of phenomena matches that of natural magnetospheres.

It is evident that an MHD-approach cannot give a fully satisfactory explanation of the M2P2 magnetosphere because a large part of it is in a non-MHD regime. But how wrong can the MHD approach be? And how much of the difference of a factor 10^{-10} in the forces on the magnetopause and on the spacecraft can be filled by considering other effects? A distributed current system within the thick non-MHD boundary layer of the artificial magnetosphere may contribute a factor of order of unity, or perhaps ten, but not ten orders of magnitude. The idea of a partial closure of the magnetopause currents near the spacecraft has been proposed in various discussions. However, our analysis shows that strong currents have to flow only a few centimeters from the spacecraft for any reasonable plasma parameters. But to really calculate the effects of the currents inside the M2P2 magnetosphere would require a very advanced computer simulation and, if negative, the results would always leave some room for doubt. Physics is an empirical science and ultimately only a rather complete space-based experiment would give the final verdict. However, considering the odds for success, it may be difficult to motivate an investment in such an experiment before more mature theoretical modelling has been made.

On the other hand, the PFMP is basically a sound idea. It would quite likely work if the superconductors would develop a bit further from the present state, or if someone would invent a practical way to construct a small, light-weigth, and steerable solar shield for the coil to assist its passive cooling.

Finally, we do not want to leave the reader with a feeling that further studies of artificial magnetospheres would be complete waste of resources. In fact, there are several interesting and potentially useful things to learn about deployment of plasma in strong magnetic fields, interactions between plasma and strongly magnetized bodies, shielding of spacecraft with plasma clouds, re-entry of spacecraft to the atmosphere, and so on.

List of Acronyms

AMSC	American Superconductor
CCC	Coated Conductor Composite
CRCD	Coil Radius vs. Current Density plot
ESA	European Space Agency
FMI	Finnish Meteorological Institute
HTS	High-Temperature Superconductors
LTS	Low-Temperature Superconductors
LISA	Laser Interferometry Space Antenna
MFC	Multi-filamentary Composite
MHD	Magnetohydrodynamics
MOD	liquid-Metal-Organic Deposition
M2P2	Mini-Magnetospheric Plasma Propulsion
NEAR	Near Earth Asteroid Rendezvous
NLR	Near Laser Rangefinder
PFMP	Plasma-free Magnetospheric Propulsion
PLR	Pulsed Laser Rangefinder
RMF	Rotating Magnetic Field
WP	Work Package

Related WWW-pages

http://www.geophys.washington.edu/Space/SpaceModel/M2P2/

http://www.islandone.org/APC/Sails/03.html

http://fuse.pha.jhu.edu/ danforth/magsail/magsail.html

http://www.magnetsales.com/Design/DesignG.htm

http://www.onera.fr/dmph-en/accelerometre/index.html

http://www.amsuper.com/html/

http://www.magnetic-shield.com/shielding.html

http://www.msss.com/small_bodies/near_new/nlr.html

http://www-ssc.igpp.ucla.edu/polar/mfedescrip.html

http://www.jsc.nasa.gov/bu2/SVLCM.html

ftp://sierra.spasci.com/DATA/timas/TIMAS_description.html

References

[*Anderson et al.,* 2002] Anderson, J. D., P. A. Laing, E. L. Lau, A. S. Lui, M. M. Nieto, and S G. Turyshev, Study of the anomalous acceleration of Pioneer 10 and 11, *Phys. Rev. D, 65*, article 082004, 2002.

[*Gilliand et al.,* 1998] Gilliand, J., R. Breun, and N. Hershkowitz, Natural pumping in a helicon discharge, *Plasma Sources Sci. and Technol.,* 7, 41, 1998.

[*Janhunen and Koskinen,* 1997] Janhunen, P., and H.E.J. Koskinen, The closure of Region-1 field-aligned current in MHD simulation, *Geophys. Res. Lett., 24*, 1419 , 1997.

[*Miljak and Chen,* 1998] Miljak, D. G., and F. F. Chen, Density limit in heliscon discharges, *Plasma Sources Sci. and Technol.,* 7, 537, 1998.

[*Minami et al.,* 1993] , Minami, S., A. I. Podgorny, and I. M. Podgorny, Laboratory evidence of earthward electric field in the magnetotail current sheet, *Geophys. Res. Lett.,* 20, 9–12, 1993.

[*Priest,* 1982] , Priest, E. R., Solar Magnetohydrodynamics, Reidel, Dordrecht, 1982.

[*Rahman et al.,* 1989] , Rahman, H. U., G. Yur, G. Wong, and R. S. White, Laboratory simulation of the large-scale Birkeland current system in the polar region with northward interplanetary magnetic field, *J. Geophys. Res.,* 94, 6873–6878, 1989.

[*Slough and Miller,* 2000] , Slough, J. T., and K. E. Miller, Flux generation and sustainment of a Field Reversed Configuration (FRC) with Rotating Magnetic Field (RMF) current drive, *Physics of Plasmas,* 7, 1495, 2000.

[*Winglee,* 1998a] Winglee, R. M., Multi-fluid simulations of the magnetosphere: The indentification of the geopause and its variation with IMF, *Geophys. Res. Lett., 25*, 4441–4444, 1998a.

[*Winglee,* 1998b] Winglee, R. M., Imaging the ionopsheric and solar wind sources in the magnetosphere through multi-fluid global simulations,Phys. Space Plasmas, 15, 345, 1998b.

[*Winglee et al.,* 2000] Winglee, R. M., J. Slough, T. Ziemba and A. Goodson, Mini-magnetospheric plasma propulsion: tapping the energy of the solar wind for spacecraft propulsion, *J. Geophys. Res.,* 105, 21067, 2000.

[*Winglee et al.,* 2001] , Winglee, R.M., T. Ziemba, J. Slough, P. Euripides, and D. Gallagher, *Space Technology and Applications International Forum-2000,* edited by M. S. El-Genk, American Institute of Physics CP552, 1-56396-980-7, p.407, 2001.

[*Ziemba et al.,* 2001] , Ziemba, T.M., R. M. Winglee, P. Euripides, and J. Slough, Parametrization of the laboratory performance of the Mini-Magnetospheric Plasma Propulsion (M2P2) prototype, *Paper IEPC-01-000 at the 27*$^{\text{th}}$ *International Electric Propulsion Conference*, Pasadena, CA, USA, 15 – 19, 2001.

[*Zubrin,* 1993] Zubrin, R.M., The use of magnetic sails to escape from low earth orbit, *J. British Interplanetary Society,* 46, 3–10, 1993.